
ALGORITHMIC RECOURSE IN THE FACE OF NOISY HUMAN RESPONSES

Martin Pawelczyk
University of Tübingen
first.last@uni-tuebingen.de

Teresa Datta
Harvard University
tdatta@g.harvard.edu

Johannes van-den-Heuvel
University of Tübingen
first.last@uni-tuebingen.de

Gjergji Kasneci
University of Tübingen
first.last@uni-tuebingen.de

Himabindu Lakkaraju
Harvard University
hlakkaraju@hbs.edu

ABSTRACT

As machine learning (ML) models are increasingly being deployed in high-stakes applications, there has been growing interest in providing recourse to individuals adversely impacted by model predictions (e.g., an applicant whose loan has been denied). To this end, several post hoc techniques have been proposed in recent literature. These techniques generate recourses under the assumption that the affected individuals will implement the prescribed recourses *exactly*. However, recent studies suggest that individuals often implement recourses in a noisy and inconsistent manner – e.g., raising their salary by \$505 if the prescribed recourse suggested an increase of \$500. Motivated by this, we introduce and study the problem of recourse invalidation in the face of noisy human responses. More specifically, we theoretically and empirically analyze the behavior of state-of-the-art algorithms, and demonstrate that the recourses generated by these algorithms are very likely to be invalidated if small changes are made to them. We further propose a novel framework, EXPECTing noisy responses (EXPECT), which addresses the aforementioned problem by explicitly minimizing the probability of recourse invalidation in the face of noisy responses. Experimental evaluation with multiple real world datasets demonstrates the efficacy of the proposed framework, and supports our theoretical findings.

1 Introduction

Over the past decade, machine learning (ML) models are increasingly being deployed to make a variety of consequential decisions in domains such as finance, healthcare, and policy. Consequently, there is growing emphasis on designing tools and techniques which can provide *recourse* to individuals who have been adversely impacted by the predictions of these models [Voigt & Von dem Bussche \(2017\)](#). For example, when an individual is denied loan by a credit scoring model employed by a bank, they should be informed about the reasons for this decision and what can be done to reverse it. When providing a recourse to an affected individual, it is critical to ensure that the corresponding decision making entity (e.g., bank) is able to honor that recourse and approve any re-application that fully implements the recommendations outlined in the prescribed recourse [Wachter et al. \(2018\)](#).

Several approaches in recent literature tackled the problem of providing recourses by generating *local* (instance level) counterfactual explanations ([Wachter et al., 2018](#); [Ustun et al., 2019](#); [Karimi et al., 2020a](#); [Poyiadzi et al., 2020](#); [Van Looveren & Klaise, 2019](#)).¹ For instance, [Wachter et al. \(2018\)](#) proposed a gradient based approach which finds the nearest counterfactual resulting in the desired prediction. [Ustun et al. \(2019\)](#) proposed an integer programming based approach to obtain *actionable* recourses for linear classifiers. More recently, [Karimi et al. \(2021, 2020c\)](#) shed light on the spuriousness of the recourses generated by counterfactual/contrastive explanation techniques [Wachter et al.](#)

¹Note that the terms counterfactual explanations ([Wachter et al., 2018](#)), contrastive explanations ([Karimi et al., 2020b](#)), and recourse ([Ustun et al., 2019](#)) are used interchangeably in prior literature. Counterfactual/contrastive explanations serve as a means to provide recourse to individuals with unfavorable algorithmic decisions. We use these terms interchangeably to refer to the notion introduced and defined by [Wachter et al. \(2018\)](#)

(2018); Ustun et al. (2019), and advocated for considering causal structure of the underlying data when generating recourses Barocas et al. (2020); Mahajan et al. (2019); Pawelczyk et al. (2020a).

The aforementioned approaches generate recourses under the assumption that the affected individuals will implement the prescribed recourses *exactly*. However, this may not always be the case in practice e.g., if recourse prescribed for an individual suggests that they increase their salary by \$500, they may reapply for a loan with a salary increment of \$505 or even \$499.95. This phenomenon of *noisy responses to prescribed recourses* is very common in the real world, and has also been noted by Björkegren et al. (2020) who conducted a field experiment in Kenya by mimicking the “digital loan” setting to study algorithmic recourse in real-world scenarios. However, it is unclear if and how often such noisy implementations of recourses would result in positive outcomes for end users. This is due to the fact that there is no prior work which attempts to understand if recourses generated by state-of-the-art approaches will remain valid (i.e., result in positive outcomes) if they are implemented in a noisy manner (i.e., small changes are made to them). In fact, our preliminary analysis (Figure 1) indicated that state-of-the-art approaches output recourses that are highly likely to be invalidated (as high as 60% of the time across multiple datasets) if small changes are made to the prescribed recourses. This poses a severe challenge to making algorithmic recourse practicable in the real world.

In this work, we introduce and address the critical problem of recourse invalidation in the face of noisy human responses. More specifically, we study if and how often recourses generated by state-of-the-art approaches become invalid (i.e., result in negative outcomes) if small changes are made to them, and provide solutions to address this problem. More specifically, we make the following key contributions:

- We formulate the problem of recourse invalidation in the face of noisy human responses to prescribed recourses.
- We carry out rigorous theoretical analysis to determine if and when recourses output by state-of-the-art approaches get invalidated (i.e., result in negative outcomes) when small changes are made to them. More specifically, we provide a closed-form expression for the probability of invalidation of the recourses output by Wachter et al. (2018). We also derive a general upper bound on the probability of invalidation of the recourses output by state-of-the-art algorithms.
- We propose a new framework called EXPECTing noisy responses (EXPECT) which generates recourses by explicitly minimizing the probability of invalidation of recourses when small changes are made to them. Our framework can ensure that the resulting recourses are invalidated at most $r\%$ of the time where r is provided as input by the end user.
- We conduct extensive experimentation with multiple real world datasets and various state-of-the-art recourse methods to validate our theoretical bounds, and also demonstrate the efficacy of our EXPECT framework.

To the best of our knowledge, this work is the first to highlight and address the problem of recourse invalidation in the face of noisy human responses. Our theoretical and empirical results clearly demonstrate that state-of-the-art approaches generate recourses that are very likely to be invalidated if users implement these recourses in a noisy fashion (i.e., make small changes to them). More specifically, we find that recourses generated by state-of-the-art approaches are invalidated up to 49% of the time when small changes are made to them (Table 1). On the other hand, recourses generated by our EXPECT framework are only invalidated up to 28% of the time (when $r = 0.35$) in the face of such noisy responses (Table 1). Note that the invalidation rates of the recourses generated by our framework can be controlled by user input, and can be reduced to arbitrarily small values by setting r to very small values. We also observe that our framework achieves high degree of robustness to noisy responses without significantly sacrificing the accuracy of the originally prescribed recourses or substantially increasing their costs. This work highlights and bridges a critical gap in the recourse literature, thereby, paving the way for real world deployment of algorithmic recourse.

2 Related Work

Our work builds on the vast literature in the field of algorithmic recourse. Below, we discuss relevant prior works and their connections to this research.

2.1 Algorithmic Approaches to Recourse

As discussed earlier, several approaches have been proposed in literature to provide recourse to individuals who have been negatively impacted by model predictions (Tolomei et al., 2017; Laugel et al., 2017; Dhurandhar et al., 2018; Wachter et al., 2018; Ustun et al., 2019; Joshi et al., 2019; Van Looveren & Klaise, 2019; Pawelczyk et al., 2020a; Mahajan et al., 2019; Mothilal et al., 2020; Karimi et al., 2020a; Rawal & Lakkaraju, 2020; Karimi et al., 2020c; Dandl et al., 2020; Antorán et al., 2021; Spooner et al., 2021). These approaches can be roughly categorized along the following dimensions Verma et al. (2020): *type of the underlying predictive model* (e.g., tree based vs. differentiable

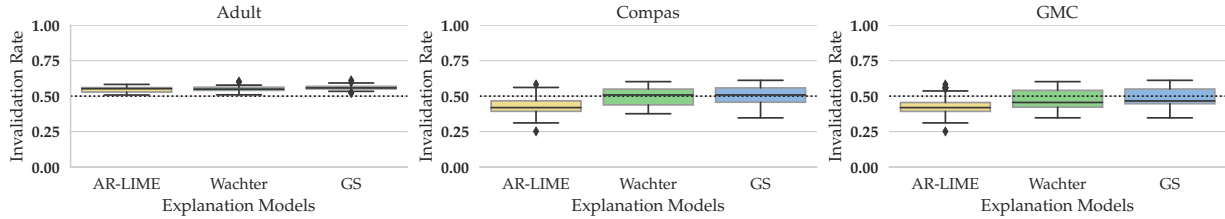


Figure 1: Boxplots of recourse invalidation rates (IR) across generated recourses \tilde{x} from the test set for Deep Neural Network (DNN) classifiers on three data sets. The recourses were generated by three different recourse methods (i.e., AR-LIME, Wachter, and GS) using CARLA (Pawelczyk et al., 2021). These methods use different techniques (i.e., integer programming, gradient search, and random search) to find minimum cost recourses. The noisy human responses were simulated by adding small Gaussian random noise $\varepsilon \sim \mathcal{N}(\mathbf{0}, 0.05 \cdot \mathbf{I})$ to \tilde{x} , where \mathbf{I} is the identity matrix. The recourse invalidation rates are as high as 60% across all datasets.

classifier), *type of access* they require to the underlying predictive model (e.g., black box vs. gradients), whether they encourage *sparsity* in counterfactuals (i.e., only a small number of features should be changed), whether counterfactuals should lie on the *data manifold*, whether the underlying *causal relationships* should be accounted for when generating counterfactuals, whether the output produced by the method should be *multiple diverse counterfactuals* or a single counterfactual, and whether the underlying *task* is posed as a regression or classification problem.

The aforementioned approaches generate recourses by implicitly assuming that the prescribed recourses will be correctly implemented by the end users. Our work, in contrast, addresses the problem of generating recourses that can be robust to noisy implementations by end users.

2.2 Robustness of Algorithmic Recourse

Prior works have focused on determining the extent to which recourses remain robust to the choice of the underlying model (Pawelczyk et al., 2020b; Black et al., 2021), shifts or changes in the underlying models (Rawal et al., 2021; Upadhyay et al., 2021), or small perturbations to the input instances (Artelt et al., 2021; Dominguez-Olmedo et al., 2021; Slack et al., 2021).

The work by Pawelczyk et al. (2020b) provides an analysis of the extra cost associated with algorithmic recourse under *model multiplicity*. For this setting, Black et al. (2021) suggest a novel sampling procedure to find recourses that can handle model multiplicity. Rawal et al. (2021), on the other hand, demonstrated theoretically and empirically that recourses generated by state-of-the-art approaches become invalid when the underlying model is updated. To address this problem, Upadhyay et al. (2021) proposed a new minimax objective to generate recourses that are robust to model updates. Artelt et al. (2021); Dominguez-Olmedo et al. (2021) consider the setting in which the input instance for which recourse is being computed may itself be noisy. Both works derive upper bounds on the recourse costs, while the latter work focuses on the causal recourse setting. Dominguez-Olmedo et al. (2021) also formulate a minimax objective to find recourses that are robust to noisy inputs. More recently, Slack et al. (2021) demonstrate how adversaries can manipulate the recourse generation process by designing an attack to generate fundamentally different recourses based on slightly different initial conditions. We also refer to Mishra et al. (2021) for a brief survey on that topic.

While prior research has focused on understanding if and how recourses generated by state-of-the-art approaches can be robust to shifts in the underlying models (Upadhyay et al., 2021; Rawal et al., 2021) or changes to the input features of individuals (Dominguez-Olmedo et al., 2021), there is no prior work that studies if and how users can obtain positive outcomes even if their implementations of (or responses to) the prescribed recourses are off by a small amount. Our work is the first to tackle this problem.

3 Preliminaries

Here, we first discuss the generic formulation leveraged by several state-of-the-art recourse methods including Wachter et al. (2018). We then define the notion of recourse invalidation rate formally.

3.1 Algorithmic Recourse: General Formulation

Notation Let $h : \mathcal{X} \rightarrow \mathcal{Y}$ denote a classifier which maps features $\mathbf{x} \in \mathcal{X} \subseteq \mathbb{R}^d$ to labels \mathcal{Y} . Let $\mathcal{Y} = \{0, 1\}$ where 0 and 1 denote an unfavorable outcome (e.g., loan denied) and a favorable outcome (e.g., loan approved), respectively.

Counterfactual (CF) explanation methods provide recourses by identifying which attributes to change for reversing an unfavorable model prediction. While several of these methods incorporate distance metrics (e.g., ℓ_p -norm) or user preferences (Rawal & Lakkaraju, 2020) to find the desired counterfactuals, some works also impose causal (Karimi et al., 2020c) or data manifold constraints (Joshi et al., 2019; Pawelczyk et al., 2020a) to find realistic counterfactuals. We now describe the generic formulation leveraged by several state-of-the-art recourse methods including Wachter et al. (2018).

Since counterfactuals that propose changes to features such as gender are not actionable, we restrict the search space to ensure that only actionable changes are allowed. Let \mathcal{A} denote the set of actionable counterfactuals. For a given predictive model h , and a predefined cost function $d_c : \mathbb{R}^d \rightarrow \mathbb{R}_+$, the problem of finding a counterfactual explanation $\tilde{\mathbf{x}} = \mathbf{x} + \delta$ for an instance $\mathbf{x} \in \mathbb{R}^d$ can be expressed by the following optimization problem:

$$\tilde{\mathbf{x}} = \arg \min_{\mathbf{x}' \in \mathcal{A}} \mathcal{L}_1(h(\mathbf{x}'), 1) + \lambda \cdot d_c(\mathbf{x}, \mathbf{x}') \quad (1)$$

where $\lambda \geq 0$ is a trade-off parameter, and $\mathcal{L}_1(\cdot, \cdot)$ is the mean-squared-error (MSE) loss. The first term on the right-hand-side ensures that the model prediction corresponding to the counterfactual i.e., $h(\mathbf{x}')$ is close to the favorable outcome label 1. The second term encourages low-cost recourses; for example, Wachter et al. (2018) propose ℓ_1 or ℓ_2 distances to ensure that the distance between the original instance \mathbf{x} and the counterfactual $\tilde{\mathbf{x}}$ is small.

3.2 Defining the Recourse Invalidation Rate

One of the key goals of this work is to understand if and when recourses output by state-of-the-art methods get invalidated when small changes are made to them. To this end, we formally define the notion of Recourse Invalidation Rate (IR) in this section.

We first introduce two key terms, namely, *prescribed recourses* and *implemented recourses*. A prescribed recourse is a recourse that was provided to an end user by some recourse method (e.g., increase salary by \$500). An implemented recourse corresponds to the recourse that the end user finally implemented (e.g., salary increment of \$505) upon being provided with the prescribed recourse. With this basic terminology in place, we now proceed to formally define Recourse Invalidation Rate (IR) below.

Definition 1 (Recourse Invalidation Rate). *For a given classifier h , the recourse invalidation rate corresponding to the counterfactual $\tilde{\mathbf{x}}_E = \mathbf{x} + \delta_E$ output by a recourse method E is given by:*

$$\Delta(\tilde{\mathbf{x}}_E; \Sigma) = \mathbb{E}_\varepsilon \left[\underbrace{h(\tilde{\mathbf{x}}_E)}_{\text{CF class}} - \underbrace{h(\tilde{\mathbf{x}}_E + \varepsilon)}_{\text{class after response}} \right], \quad (2)$$

where the expectation is taken with respect to a Gaussian random variable $\varepsilon \sim \mathcal{N}(\mathbf{0}, \Sigma)$ which captures the noise in human responses.

Since the implemented recourses do not typically match the prescribed recourses, we add noise ε to the prescribed recourse $\tilde{\mathbf{x}}_E$. Since we primarily compute recourses for individuals \mathbf{x} such that $h(\mathbf{x}) = 0$, the label corresponding to the counterfactual is given by $h(\tilde{\mathbf{x}}_E) = 1$ and therefore $\Delta \in [0, 1]$. For example, the following cases help understand our Recourse Invalidation Rate metric better: When $\Delta = 0$, then the prescribed recourse and the recourse implemented by the user agree all the time; when $\Delta = 0.5$, the prescribed recourse and the implemented recourse agree half of the time, and finally, when $\Delta = 1$ then the prescribed recourse and the recourse implemented by the user never agree. Figure 2, and Figure 7 from Appendix A provide further intuition about our IR metric. Note that our IR metric leverages a Gaussian random variable ε to model the noise in human responses.

4 Our Theoretical Analysis

In this section, we theoretically analyze the recourse invalidation rates (IRs) of state-of-the-art recourse methods. More specifically: 1) we provide a closed-form expression for the IR corresponding to any instance, 2) using the above

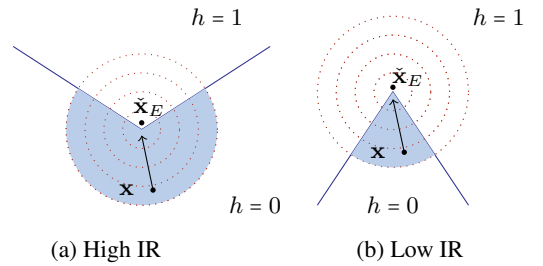


Figure 2: Recourse invalidation rates (IRs) (blue area). The blue line indicates the decision boundary, \mathbf{x} is the original input, and $\tilde{\mathbf{x}}_E$ is the generated recourse. The shaded region ($h = 0$) belongs to the negative class, and the unshaded region ($h = 1$) to the positive class. Figure 2a demonstrates the case where recourse invalidation rate for $\tilde{\mathbf{x}}_E$ is high because small perturbations to $\tilde{\mathbf{x}}_E$ are more likely to end up in the shaded region (negative class). Figure 2b demonstrates the case where recourse invalidation rate for $\tilde{\mathbf{x}}_E$ is low because small perturbations to $\tilde{\mathbf{x}}_E$ are less likely to end up in the shaded region.

closed-form expression, we analyze one of the most popular recourse methods [Wachter et al. \(2018\)](#) proving that additional cost has to be incurred to generate robust recourses in the face of noisy human responses, and 3) we derive a general upper bound on the IR which is applicable to any valid recourse provided by any method with the underlying classifier being a differentiable model.

4.1 A Closed-Form Expression for Recourse Invalidation Rate

Before we introduce our formal result, we define $h(\mathbf{x})=g(f(\mathbf{x}))$, where $f: \mathcal{X} \rightarrow \mathbb{R}$ is a differentiable scoring function (e.g., logit scoring function) and $g: \mathbb{R} \rightarrow \mathcal{Y}$ an activation function that maps logit scores to binary labels. Throughout the remainder of this work we will use $g(u) = \mathbb{I}[u > \xi]$, where ξ is a decision rule in logit space. W.l.o.g. we will set $\xi = 0$.

Here, we use definition 1 and provide a closed-form expression for the IR. We solve for the IR for a local approximation of the true model. The procedure suggested here remains generalizable even for non-linear models since the local behavior of a given non-linear model can often be well approximated by fitting a locally linear model ([Ribeiro et al., 2016](#)). Moreover, note that these approximations have already been leveraged successfully by existing approaches from the algorithmic recourse literature ([Ustun et al., 2019](#); [Upadhyay et al., 2021](#); [Rawal & Lakkaraju, 2020](#)).

Theorem 1 (Closed-Form Recourse Invalidation Rate). *A first-order approximation $\tilde{\Delta}$ to the recourse invalidation rate Δ in (2) under a Gaussian distribution $\varepsilon \sim \mathcal{N}(\mathbf{0}, \Sigma)$ capturing the noise in human responses is given by:*

$$\tilde{\Delta}(\tilde{\mathbf{x}}_E; \Sigma) = 1 - \Phi\left(\frac{f(\tilde{\mathbf{x}}_E)}{\sqrt{\nabla f(\tilde{\mathbf{x}}_E) \Sigma \nabla f(\tilde{\mathbf{x}}_E)^T}}\right), \quad (3)$$

where Φ is the CDF of the univariate standard normal distribution $\mathcal{N}(0, 1)$, $f(\tilde{\mathbf{x}}_E)$ denotes the logit score at $\tilde{\mathbf{x}}_E$ which is the recourse output by a recourse method E , and $h(\tilde{\mathbf{x}}_E) \in \{0, 1\}$.

Proof Sketch. The proof uses the definition of the recourse invalidation rate and evaluates the expectation $\mathbb{E}_\varepsilon[\mathbb{I}[f(\tilde{\mathbf{x}}_E + \varepsilon) > 0]]$, where we have used the fact that there is a 1-to-1 correspondence between the logit score $f(\tilde{\mathbf{x}}_E)$ and the corresponding probabilistic outcome. We then leverage results on combinations of Gaussian random variables. The full proof is given in Appendix D.1. \square

This result is intuitive. First, when $f(\tilde{\mathbf{x}}_E) = 0$, then $\Delta = 0.5$ since $\Phi(0) = \frac{1}{2}$. This means that the prescribed recourse and the recourse implemented by the user *agree 50% of the time*. We depicted this case in Figure 3. Second, when $f(\tilde{\mathbf{x}}_E) \rightarrow +\infty$, then $\Delta \rightarrow 0$ since $\Phi \rightarrow 1$, which means that the prescribed recourse and the recourse implemented by the user *always agree*. Finally, we consider the impact of the variance $\Sigma = \sigma^2 \mathbf{I}$. If σ^2 decreases, then the size of the neighborhood where the recourse has to be robust shrinks, and therefore our IR $\Delta \rightarrow 0$ as $\sigma^2 \rightarrow 0$ if $f(\tilde{\mathbf{x}}_E) \geq 0$. The expression in (3) is a key ingredient required for both the algorithm presented in Section 5 and our results that follow next.

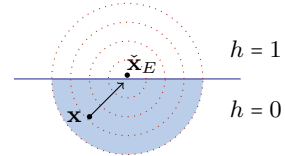


Figure 3: The recourse invalidation rate (blue area) for a locally linear decision boundary, where the noisy responses follow $\mathcal{N}(\tilde{\mathbf{x}}_E, \sigma^2 \mathbf{I})$. The blue line is the decision boundary. \mathbf{x} is the original input, and $\tilde{\mathbf{x}}_E$ is the prescribed recourse. The shaded region ($h = 0$) belongs to the negative class, and the unshaded region ($h = 1$) to the positive class. Figure demonstrates the case where recourse invalidation rate for $\tilde{\mathbf{x}}_E$ is 0.5 because small perturbations to $\tilde{\mathbf{x}}_E$ are equally likely to end up in either the shaded region (negative class) or the unshaded region (positive class).

4.2 Recourse Invalidation Rate for [Wachter et al. \(2018\)](#)

Next, we specify the recourse invalidation rate for the algorithm proposed by [Wachter et al. \(2018\)](#). For their algorithm, [Pawelczyk et al. \(2022\)](#) give a closed-form recourse solution for logistic regression classifiers when $d_c = \|\mathbf{x} - \mathbf{x}'\|_2$ and the MSE-loss is used. Then the solution takes the following form: $\tilde{\mathbf{x}}_{\text{Wachter}}(s) = \mathbf{x} + \frac{s - f(\mathbf{x})}{\|\nabla f(\mathbf{x})\|_2} \nabla f(\mathbf{x})$, where s is the target logit score. More specifically, to arrive at the desired class with probability of 0.5, the target score for a sigmoid function is $s = 0$, where the logit corresponds to a 0.5 probability for $y = 1$. The next statement quantifies the IR of recourses output by [Wachter et al. \(2018\)](#).

Lemma 1. *For the logistic regression classifier, consider the recourse output by [Wachter et al. \(2018\)](#): $\tilde{\mathbf{x}}_{\text{Wachter}}(s) = \mathbf{x} + \frac{s - f(\mathbf{x})}{\|\nabla f(\mathbf{x})\|_2} \nabla f(\mathbf{x})$. Then the recourse invalidation rate has the following closed-form:*

$$\Delta(\tilde{\mathbf{x}}_{\text{Wachter}}(s); \sigma^2 \mathbf{I}) = 1 - \Phi\left(\frac{s}{\sigma \|\nabla f(\mathbf{x})\|_2}\right), \quad (4)$$

Algorithm 1 EXPECT

Input: \mathbf{x} s.t. $f(\mathbf{x}) < 0$, $f, \Sigma, \lambda > 0$, Learning rate: $\alpha > 0$
Initialize: $\mathbf{x}' = \mathbf{x}$; $\tilde{\Delta} = \text{ClosedFormIR}(f, \Sigma, \mathbf{x})$
while $\tilde{\Delta} > r$ **and** $f(\mathbf{x}') < 0$ **do**
 $\hat{\Delta} = \text{ClosedFormIR}(f, \Sigma, \mathbf{x}')$ {from Thm. 1}
 $\mathbf{x}' = \mathbf{x}' - \alpha \cdot \nabla_{\mathbf{x}'} \mathcal{L}(\mathbf{x}'; \Sigma, r, \lambda)$ {Optimize (7)}
end while
Return: $\check{\mathbf{x}} = \mathbf{x}'$

where s is the target logit score.

Proof Sketch. The proof uses the recourse expression from Pawelczyk et al. (2022) and plugs it into (3). \square

A recourse generated by Wachter et al. (2018) such that $f(\check{\mathbf{x}}_{\text{Wachter}}) = s = 0$ will result in $\Delta = 0.5$. Note that this is true regardless of the choice of Σ . To obtain recourse that is more robust to noisy responses from users, i.e., $\Delta \rightarrow 0$, the decision maker can choose a higher logit target score of $s' > s \geq 0$ since this decreases the recourse invalidation rate, i.e., $\Delta(\check{\mathbf{x}}_{\text{Wachter}}(s)) > \Delta(\check{\mathbf{x}}_{\text{Wachter}}(s'))$.² Thus, we can now see that there exists a trade-off between robustness to noisy human responses and cost: since $\|\check{\mathbf{x}}_{\text{Wachter}}(s')\| > \|\check{\mathbf{x}}_{\text{Wachter}}(s)\|$ while $\Delta(\check{\mathbf{x}}_{\text{Wachter}}(s')) < \Delta(\check{\mathbf{x}}_{\text{Wachter}}(s))$, we see that a higher target score leads to a more robust recourse, while increasing the recourse costs holding all other variables constant (e.g. \mathbf{x} and σ^2).

4.3 A General Upper Bound on the Recourse Invalidation Rate

Next, we derive a general upper bound on the recourse invalidation rate. This bound is applicable to any method E that provides recourses resulting in a positive outcome.

Lemma 2. *Let $\check{\mathbf{x}}_E$ be the output produced by some recourse method E such that $h(\check{\mathbf{x}}_E) = 1$. Then, an upper bound on $\tilde{\Delta}$ from (3) is given by:*

$$\tilde{\Delta}(\check{\mathbf{x}}_E; \sigma^2 \mathbf{I}) \leq 1 - \Phi\left(c + \frac{\omega}{\sigma} \frac{\|\nabla f(\mathbf{x})\|_2}{\|\nabla f(\check{\mathbf{x}}_E)\|_2} \frac{\|\delta_E\|_1}{\sqrt{\|\delta_E\|_0}}\right), \quad (5)$$

where $c = \frac{f(\mathbf{x})}{\sigma \cdot \|\nabla f(\mathbf{x})\|_2}$ is a constant, $\delta_E = \check{\mathbf{x}}_E - \mathbf{x}$, and $\omega > 0$ is the cosine of the angle between the vectors $\nabla f(\mathbf{x})$ and δ_E .

Proof Sketch. Starting from (3), we use the approximation of $f(\check{\mathbf{x}}_E)$ in combination with the fact that $\omega = \frac{\nabla f(\mathbf{x})^T \delta_E}{\|\delta_E\|_2 \cdot \|\nabla f(\mathbf{x})\|_2}$. We conclude using a lower bound on the ℓ_2 -norm of δ_E which depends on both its ℓ_0 and ℓ_1 -norms. \square

The right term in the inequality entails that the upper bound depends on the ratio of the ℓ_1 and ℓ_0 -norms of the recourse action δ_E provided by recourse method E . The higher the ℓ_1/ℓ_0 ratio of the recourse actions, the tighter the bound. The bound is tight when $\|\delta_E\|_0$ assumes minimum value i.e., $\|\delta_E\|_0 = 1$ since at least one feature needs to be changed to flip the model prediction.

5 Our Framework: EXPECT

So far, we have discussed how recourses generated by existing methods are not robust to noisy human responses. Here, we present our framework, EXPECTing noisy responses, which will enable us to generate robust recourses by design. We introduce our objective function, which is followed by a discussion on how to operationalize and optimize it efficiently.

5.1 Formulating and Optimizing our Objective

Our Objective The main idea is to find a recourse suggestion $\check{\mathbf{x}}$ whose prediction at any point \mathbf{y} within some set around $\check{\mathbf{x}}$ belongs to the positive class with probability r . Hence, our idea consists of minimizing the recourse invalidation rate

²This is not generally true in non-linear models.

subject to the constraint of low cost recourse. Our objective looks as follows:

$$\tilde{\mathbf{x}} = \arg \min_{\mathbf{x}' \in \mathcal{A}} \Delta(\mathbf{x}'; \Sigma) \text{ s.t. } d_c(\mathbf{x}, \mathbf{x}') \leq q \wedge h(\mathbf{x}') \neq 0, \quad (6)$$

where q is a cost budget, $\Delta(\mathbf{x}'; \Sigma)$ is the recourse invalidation rate from (1), d_c measures the distance between the factual input and the prescribed recourse, and h is the fixed classifier. We use a Lagrangian formulation with parameter λ to encourage balance between the different objectives as follows:

$$\mathcal{L} = \mathcal{L}_0(\mathbf{x}'; \Sigma) + \mathcal{L}_1(f(\mathbf{x}'), s) + \lambda \cdot d_c(\mathbf{x}', \mathbf{x}), \quad (7)$$

where $\mathcal{L}_0 = \max(0, \Delta(\mathbf{x}'; \Sigma) - r)$ and r is the target IR. The new component \mathcal{L}_0 is a Hinge loss encouraging that the prescribed recourse has a low probability of invalidation, and the parameter Σ controls the shape and the size of the neighbourhood in which the recourse has to be robust in line with Definition 1. In practical use-cases the choice of r would depend on the risk-aversion of the end-user. If the end-user is not confident about achieving a ‘precision landing’, then a rather low invalidation target should be chosen (i.e., $r < 0.5$). In the extreme case, when $r = 0$, the objective would encourage finding recourses that always lead to a positive outcome for a given neighborhood shape and size controlled by Σ .

Optimization We suggest two ways to minimize the objective in (7). First, we can approximate the IR in (2) (i.e., Δ) by replacing it with the approximate closed-form IR expression $\tilde{\Delta}$ from (3) and minimize (7). Algorithm 1 then proceeds in an iterative fashion where we do gradient descent on the loss function in (7). This procedure is executed repeatedly until the class label flips from 0 to 1 and $\tilde{\Delta}$ is less than or equal to r . Second, instead of using (3) we can use a Monte-Carlo approach in combination with the *reparametrization trick* to obtain a differentiable approximation of IR. Intuitively, this trick separates the randomness of the noise distribution and the influence of the distribution parameters with respect to which we want to take the gradients. We refer to Kingma & Welling (2013) for a detailed discussion of this trick. Our implementation provides both options. Appendix A presents an extension of our framework to obtain reliable recourses for non-differentiable tree-based classifiers.

Synthetic Example In Figure 4, we demonstrate how EXPECT finds recourses relative to Wachter’s algorithm. We see that EXPECT finds recourses in line with both the chosen invalidation target (e.g., in the left panel the target is set $r = 0.3$) and the variance σ^2 which controls the size of the neighborhood, in which the recourses have to be robust. We show a similar example in Figure 7 of Appendix A, which demonstrates how EXPECT works on tree-based models.

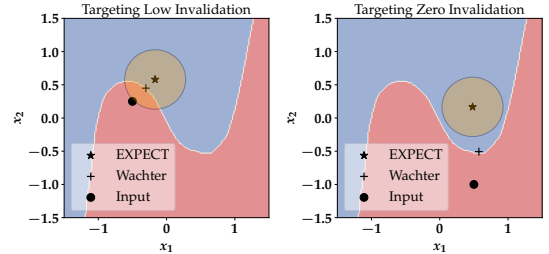


Figure 4: Computing recourses with low IRs on the binary classification *moon data set* (Pedregosa et al., 2011) for a NN classifier with 100 hidden units. The circles around EXPECT’s recourses have radius 2σ , i.e., they show the region where 95% of recourse inaccuracies fall when $\sigma^2 = 0.05$. **Left:** We chose an invalidation target of $r = 0.3$, i.e., 30% of the recourse responses would fail under spherical response inaccuracies $\varepsilon \sim \mathcal{N}(\mathbf{0}, 0.05 \cdot \mathbf{I})$. **Right:** The same setup as on the left, but now we chose $r = 0$.

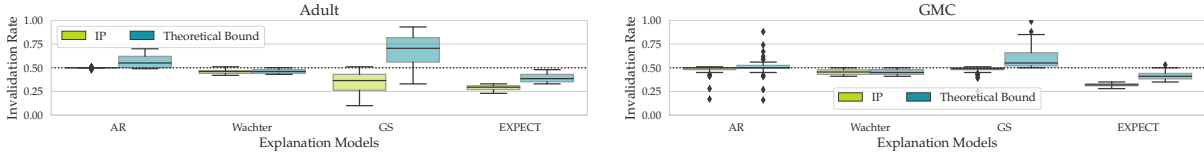
6 Experimental Evaluation

We now present our empirical analysis. First, we validate our theoretical results on the recourse invalidation rates across various recourse methods. Second, we study the effectiveness of EXPECT at finding robust recourses in the presence of noisy human responses.

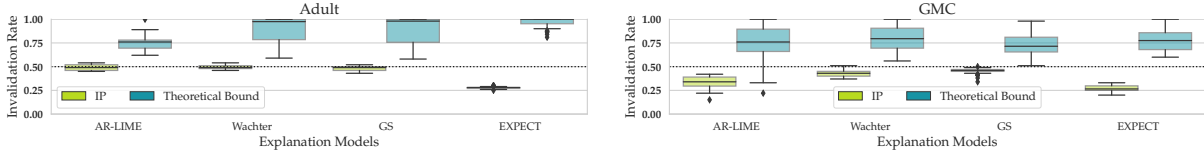
6.1 Experimental Setup

We first describe the various synthetic and real-world data sets leveraged in our experimentation. We then describe the predictive models that we employ in our experiments, and the various state-of-the-art recourse methods that we utilize as baselines.

Real-World Data and Noisy Responses Regarding real-world data, we use the same data sets as provided in the recourse and counterfactual explanation library CARLA (Pawelczyk et al., 2021). The *Adult* data set Dua & Graff (2017) originates from the 1994 Census database, consisting of 14 attributes and 48,842 instances. The class label indicates whether an individual has an income greater than 50,000 USD/year. The *Give Me Some Credit* (GMC) data set Kaggle-Competition (2011) is a credit scoring data set, consisting of 150,000 observations and 11 features. The class label indicates if the corresponding individual will experience financial distress within the next two years (*SeriousDlqin2yrs* is 1) or not. The *COMPAS* data set Angwin et al. (2016) contains data for more than 10,000 criminal defendants in Florida. It is used by the jurisdiction to score defendant’s likelihood of re-offending. The class label indicates if the corresponding defendant is high or low risk for recidivism. All the data sets were normalized so



(a) Logistic Regression, $\sigma^2 = 0.01$



(b) Neural Network, $\sigma^2 = 0.01$

Figure 5: Verifying the theoretical upper bound from Lemma 2 for the logistic regression and deep neural network classifiers on the Adult and GMC data sets when $\sigma^2 = 0.01$. The green boxplots show the empirical recourse invalidation rates for AR(-LIME), Wachter, GS, and EXPECT ($r = 0.35$). The blue boxplots show the distribution of upper bounds, which we evaluated by plugging in the corresponding quantities (i.e., σ^2 , ω , etc.) into the upper bound from Lemma 2. The results show no violations of our theoretical bounds. We refer to Appendix C for the full set of experimental results.

that $\mathbf{x} \in [0, 1]^d$. Across all experiments, we add noise ε to the prescribed recourse $\tilde{\mathbf{x}}_E$, where $\varepsilon \sim \mathcal{N}(\mathbf{0}, \sigma^2 \cdot \mathbf{I})$ and $\sigma^2 \in \{0.01, 0.025, 0.05\}$.

Methods We compare the recourses generated by EXPECT to three different methods which aim to generate low-cost recourses using fundamentally different principles: AR (-LIME) uses an integer-programming-based objective [Ustun et al. \(2019\)](#), Wachter uses a gradient-based objective ([Wachter et al., 2018](#)), and GS is based on a random search algorithm ([Lauigel et al., 2017](#)). We have used the recourse method implementations from the CARLA library ([Pawelczyk et al., 2021](#)).

Prediction Models For all data sets (except the synthetic one), we trained both ReLU-based ANN models with 50 hidden layers and logistic regression classifiers. All recourses were generated with respect to these classifiers. We provide details on these models in Appendix B.

	Adult				Compas				GMC				
	AR	Wachter	GS	EXPECT	AR	Wachter	GS	EXPECT	AR	Wachter	GS	EXPECT	
LR	RA (\uparrow)	0.98	1.0	1.0	1.0	1.0	1.0	1.0	1.0	1.0	1.0	1.0	
	AIR (\downarrow)	0.5 ± 0.01	0.46 ± 0.02	0.35 ± 0.11	0.22 ± 0.02	0.48 ± 0.04	0.47 ± 0.02	0.3 ± 0.18	0.08 ± 0.01	0.47 ± 0.06	0.45 ± 0.03	0.48 ± 0.04	0.24 ± 0.01
	AC (\downarrow)	0.55 ± 0.4	0.62 ± 0.43	2.12 ± 1.05	1.24 ± 0.81	0.16 ± 0.17	0.22 ± 0.17	0.73 ± 0.45	0.66 ± 0.27	0.29 ± 0.27	0.49 ± 0.51	0.28 ± 0.31	1.01 ± 2.01
NN	RA (\uparrow)	0.38	1.0	1.0	1.0	0.84	1.0	1.0	1.0	0.38	1.0	1.0	1.0
	AIR (\downarrow)	0.49 ± 0.03	0.5 ± 0.02	0.48 ± 0.02	0.28 ± 0.01	0.34 ± 0.09	0.46 ± 0.02	0.43 ± 0.07	0.18 ± 0.03	0.34 ± 0.07	0.43 ± 0.03	0.45 ± 0.03	0.27 ± 0.03
	AC (\downarrow)	1.05 ± 0.22	0.3 ± 0.19	2.99 ± 1.51	1.43 ± 0.49	1.15 ± 0.52	0.2 ± 0.16	0.81 ± 0.45	0.8 ± 0.34	0.2 ± 0.19	0.26 ± 0.18	0.12 ± 0.09	0.47 ± 0.21

Table 1: Recourse accuracy (RA), average recourse invalidation rate (AIR) for $\sigma^2 = 0.01$ and average cost (AC) across different recourse methods. Recourses that use our framework EXPECT are more robust compared to those produced by existing baselines. For EXPECT, we generated recourses by setting $r = 0.35$ and $\sigma^2 = 0.01$. As a consequence, the AIR should be at most 0.35, which is in line with our results. The full set of experiments is provided in Appendix C.

6.2 Validating our Theoretical Bounds

Computing the Bounds We empirically validate the theoretical upper bounds derived in Section 4. To do that, we first estimate the bounds for each instance in the test set according to Lemma 2, and compare them with the empirical estimates of the IR. The empirical IR, in turn, we obtain from Monte-Carlo approximations of the IR in (2). We observed that 10,000 samples were sufficient to get a stable approximation of IR, i.e., increasing the number of samples to 100,000 did not change the IR estimate significantly.

Results In Figure 5, we validate the bounds obtained in Lemma 2 for the Adult and GMC data sets. We relegated results for the Compas data set and other values of σ^2 to Appendix C. Note that the trivial upper bound is 1 since $\Delta \leq 1$, and we see that our bounds usually lie well below this value, which suggests that our bounds are meaningful. For the linear models in particular, we observe that our upper bounds are quite tight, thus providing accurate estimates of the worst

case recourse invalidation rates. It is noteworthy that GS tends to provide looser bounds, since its recourses tend to have lower ℓ_1/ℓ_0 ratios; for GS, its random search procedure increases the ℓ_0 -norms of the recourse relative to the recourses output by other recourse methods. This contributes to a looser bound saying that the randomly sampled recourses by GS tend to provide looser worst-case IR estimates relative to all the other methods, which do use gradient information (i.e., Wachter, AR and EXPECT).

6.3 Evaluating the EXPECT Framework

Measures We consider three measures in our evaluation: 1) We measure the *average cost* (AC) required to act upon the prescribed recourses where the average is taken with respect to all instances in the test set for which a given method provides recourse. Since all our algorithms are optimizing for the ℓ_1 -norm we use this as our cost measure. 2) We use *recourse accuracy* (RA) defined as the fraction of instances in the test set for which acting upon the prescribed recourse results in the desired prediction. 3) We compute the *average IR* across every instance in the test set. To do that, we sample 10,000 points from $\varepsilon \sim \mathcal{N}(\mathbf{0}, \sigma^2 \mathbf{I})$ for every instance and compute IR in (2). Then the *average IR* quantifies recourse robustness where the individual IRs are averaged over all instances from the test set for which a given method provides recourse.

Results Here, we evaluate the robustness, costs and recourse accuracy of the recourses generated by our framework EXPECT relative to the baselines. We consider a recourse robust if the recourse remains valid (i.e., results in positive outcome) even after small changes are made to it (i.e., humans implement it in a noisy manner). Table 1 shows the average IR for different methods across different real world data sets and classifiers when $\sigma^2 = 0.01$. It can be seen that EXPECT has the lowest invalidation rate across all real-world data sets and classifiers. We also consider if the robustness achieved by our framework is associated with an additional cost i.e., by sacrificing recourse accuracy (RA) or by increasing the average recourse cost (AC). We compute AC of the recourses output by all the algorithms on various data sets and find that EXPECT usually has the highest or second highest recourse costs, while the recourse accuracy is at 100% across classifiers and data sets. Finally, in Figures 13, 14, and 15 from Appendix C we show that the IRs of the recourses by our framework can be controlled setting r to desired values.

7 Conclusion

In this work, we introduced and studied the critical problem of recourse invalidation in the face of noisy human responses. More specifically, we theoretically and empirically analyzed the behavior of state-of-the-art recourse methods, and demonstrated that the recourses generated by these methods are very likely to be invalidated if small changes are made to them. We further proposed a novel framework, EXPECTing noisy responses (EXPECT), which addresses the aforementioned problem by explicitly minimizing the probability of recourse invalidation in the face of noisy responses. Experimental evaluation with multiple real world datasets not only demonstrated the efficacy of the proposed framework, but also validated our theoretical findings. Our work also paves the way for several interesting future research directions in the field of algorithmic recourse. For instance, it would be interesting to build on this work to develop approaches which can generate recourses that are simultaneously robust to noisy human responses, noise in the inputs, as well as shifts in the underlying models. It would also be important to understand the trade-offs involved in achieving these different kinds of robustness.

References

- Angwin, J., Larson, J., Mattu, S., and Kirchner, L. Machine bias: There’s software used across the country to predict future criminals. and it’s biased against blacks, 2016.
- Antorán, J., Bhatt, U., Adel, T., Weller, A., and Hernández-Lobato, J. M. Getting a clue: A method for explaining uncertainty estimates. In *International Conference on Learning Representations (ICLR)*, 2021.
- Artelt, A., Vaquet, V., Velioglu, R., Hinder, F., Brinkrolf, J., Schilling, M., and Hammer, B. Evaluating robustness of counterfactual explanations. *arXiv:2103.02354*, 2021.
- Barocas, S., Selbst, A. D., and Raghavan, M. The hidden assumptions behind counterfactual explanations and principal reasons. In *Proceedings of the Conference on Fairness, Accountability, and Transparency (FAT*)*, New York, NY, USA, 2020. ACM.
- Björkegren, D., Blumenstock, J. E., and Knight, S. Manipulation-proof machine learning. *arXiv:2004.03865*, 2020.
- Black, E., Wang, Z., Fredrikson, M., and Datta, A. Consistent counterfactuals for deep models. *arXiv:2110.03109*, 2021.

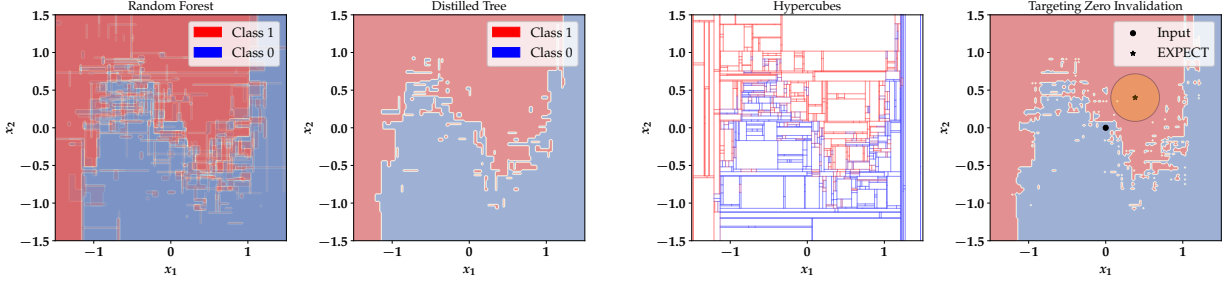
- Borisov, V., Leemann, T., Seßler, K., Haug, J., Pawelczyk, M., and Kasneci, G. Deep neural networks and tabular data: A survey. *arXiv:2110.01889*, 2021.
- Breiman, L. Random forests. *Machine learning*, 45(1):5–32, 2001.
- Bucilua, C., Caruana, R., and Niculescu-Mizil, A. Model compression. In *Proceedings of the 12th ACM SIGKDD international conference on Knowledge discovery and data mining (KDD)*, 2006.
- Dandl, S., Molnar, C., Binder, M., and Bischl, B. Multi-objective counterfactual explanations. In *International Conference on Parallel Problem Solving from Nature*, pp. 448–469. Springer, 2020.
- Dhurandhar, A., Chen, P.-Y., Luss, R., Tu, C.-C., Ting, P., Shanmugam, K., and Das, P. Explanations based on the missing: Towards contrastive explanations with pertinent negatives. In *Advances in Neural Information Processing Systems (NeurIPS)*, 2018.
- Domingos, P. Knowledge acquisition from examples via multiple models. In *14th International Conference on Machine Learning*, pp. 98–106, 1997.
- Dominguez-Olmedo, R., Karimi, A.-H., and Schölkopf, B. On the adversarial robustness of causal algorithmic recourse. *arXiv:2112.11313*, 2021.
- Dua, D. and Graff, C. UCI machine learning repository, 2017.
- Friedman, J. H. Greedy function approximation: a gradient boosting machine. *Annals of statistics*, pp. 1189–1232, 2001.
- Hinton, G., Vinyals, O., and Dean, J. Distilling the knowledge in a neural network. *arXiv:1503.02531*, 2015.
- Joshi, S., Koyejo, O., Vijitbenjaronk, W., Kim, B., and Ghosh, J. Towards realistic individual recourse and actionable explanations in black-box decision making systems. *arXiv:1907.09615*, 2019.
- Kaggle-Competition. "give me some credit data set", 2011.
- Karimi, A.-H., Barthe, G., Balle, B., and Valera, I. Model-agnostic counterfactual explanations for consequential decisions. In *International Conference on Artificial Intelligence and Statistics (AISTATS)*, 2020a.
- Karimi, A.-H., Barthe, G., Schölkopf, B., and Valera, I. A survey of algorithmic recourse: definitions, formulations, solutions, and prospects. *arXiv:2010.04050*, 2020b.
- Karimi, A.-H., von Kügelgen, J., Schölkopf, B., and Valera, I. Algorithmic recourse under imperfect causal knowledge: a probabilistic approach. In *Conference on Neural Information Processing Systems (NeurIPS)*, 2020c.
- Karimi, A.-H., Schölkopf, B., and Valera, I. Algorithmic recourse: from counterfactual explanations to interventions. In *Proceedings of the 2021 ACM Conference on Fairness, Accountability, and Transparency*, pp. 353–362, 2021.
- Kingma, D. P. and Welling, M. Auto-encoding variational bayes. *arXiv preprint arXiv:1312.6114*, 2013.
- Laugel, T., Lesot, M.-J., Marsala, C., Renard, X., and Detyniecki, M. Inverse classification for comparison-based interpretability in machine learning. *arXiv preprint arXiv:1712.08443*, 2017.
- Lucic, A., Oosterhuis, H., Haned, H., and de Rijke, M. Focus: Flexible optimizable counterfactual explanations for tree ensembles. In *Proceedings of the AAAI Conference on Artificial Intelligence (AAAI)*, 2022.
- Mahajan, D., Tan, C., and Sharma, A. Preserving causal constraints in counterfactual explanations for machine learning classifiers. *arXiv preprint arXiv:1912.03277*, 2019.
- Mishra, S., Dutta, S., Long, J., and Magazzeni, D. A survey on the robustness of feature importance and counterfactual explanations. *arXiv:2111.00358*, 2021.
- Mothilal, R. K., Sharma, A., and Tan, C. Explaining machine learning classifiers through diverse counterfactual explanations. In *Proceedings of the Conference on Fairness, Accountability, and Transparency (FAT*)*, 2020.
- Paszke, A., Gross, S., Massa, F., Lerer, A., Bradbury, J., Chanan, G., Killeen, T., Lin, Z., Gimelshein, N., Antiga, L., et al. Pytorch: An imperative style, high-performance deep learning library. *arXiv:1912.01703*, 2019.
- Pawelczyk, M., Broelemann, K., and Kasneci, G. Learning model-agnostic counterfactual explanations for tabular data. In *Proceedings of The Web Conference 2020 (WWW)*. ACM, 2020a.
- Pawelczyk, M., Broelemann, K., and Kasneci, G. On counterfactual explanations under predictive multiplicity. In *Proceedings of the 36th Conference on Uncertainty in Artificial Intelligence (UAI)*, pp. 809–818. PMLR, 2020b.
- Pawelczyk, M., Bielawski, S., Van den Heuvel, J., Richter, T., and Kasneci, G. Carla: A python library to benchmark algorithmic recourse and counterfactual explanation algorithms. In *Advances in Neural Information Processing Systems (NeurIPS) (Benchmark and Datasets Track)*, volume 34, 2021.

- Pawelczyk, M., Agarwal, C., Joshi, S., Upadhyay, S., and Lakkaraju, H. Exploring counterfactual explanations through the lens of adversarial examples: A theoretical and empirical analysis. In *International Conference on Artificial Intelligence and Statistics (AISTATS)*, 2022.
- Pedregosa, F., Varoquaux, G., Gramfort, A., Michel, V., Thirion, B., Grisel, O., Blondel, M., Prettenhofer, P., Weiss, R., Dubourg, V., et al. Scikit-learn: Machine learning in python. *Journal of machine learning research*, 2011.
- Phuong, M. and Lampert, C. Towards understanding knowledge distillation. In *International Conference on Machine Learning (ICML)*. PMLR, 2019.
- Poyiadzi, R., Sokol, K., Santos-Rodriguez, R., De Bie, T., and Flach, P. Face: Feasible and actionable counterfactual explanations. In *Proceedings of the AAAI/ACM Conference on AI, Ethics, and Society, AIES '20*, pp. 344–350, New York, NY, USA, 2020. Association for Computing Machinery. ISBN 9781450371100. doi: 10.1145/3375627.3375850. URL <https://doi.org/10.1145/3375627.3375850>.
- Rawal, K. and Lakkaraju, H. Interpretable and interactive summaries of actionable recourses. In *Advances in Neural Information Processing Systems (NeurIPS)*, volume 33, 2020.
- Rawal, K., Kamar, E., and Lakkaraju, H. Algorithmic recourse in the wild: Understanding the impact of data and model shifts. *arXiv:2012.11788*, 2021.
- Ribeiro, M. T., Singh, S., and Guestrin, C. ” why should i trust you?” explaining the predictions of any classifier. In *Proceedings of the 22nd ACM SIGKDD international conference on knowledge discovery and data mining (KDD)*, pp. 1135–1144, 2016.
- Slack, D., Hilgard, S., Lakkaraju, H., and Singh, S. Counterfactual explanations can be manipulated. In *Advances in Neural Information Processing Systems (NeurIPS)*, volume 34, 2021.
- Spooner, T., Dervovic, D., Long, J., Shepard, J., Chen, J., and Magazzeni, D. Counterfactual explanations for arbitrary regression models. *arXiv:2106.15212*, 2021.
- Tolomei, G., Silvestri, F., Haines, A., and Lalmas, M. Interpretable predictions of tree-based ensembles via actionable feature tweaking. In *Proceedings of the ACM SIGKDD International Conference on Knowledge Discovery & Data Mining (KDD)*. ACM, 2017.
- Upadhyay, S., Joshi, S., and Lakkaraju, H. Towards robust and reliable algorithmic recourse. In *Advances in Neural Information Processing Systems (NeurIPS)*, volume 34, 2021.
- Ustun, B., Spangher, A., and Liu, Y. Actionable recourse in linear classification. In *Proceedings of the Conference on Fairness, Accountability, and Transparency (FAT*)*, 2019.
- Van Looveren, A. and Klaise, J. Interpretable counterfactual explanations guided by prototypes. *arXiv preprint arXiv:1907.02584*, 2019.
- Verma, S., Dickerson, J., and Hines, K. Counterfactual explanations for machine learning: A review. *arXiv:2010.10596*, 2020.
- Voigt, P. and Von dem Bussche, A. The eu general data protection regulation (gdpr). *A Practical Guide, 1st Ed.*, Cham: Springer International Publishing, 10:3152676, 2017.
- Wachter, S., Mittelstadt, B., and Russell, C. Counterfactual explanations without opening the black box: automated decisions and the gdpr. *Harvard Journal of Law & Technology*, 31(2), 2018.

Appendix

A Extensions to Tree Ensemble Classifiers

The recourse literature commonly considers consequential decision problems which heavily rely on the usage of tabular data. For this data modality, ensembles of decision trees such as Random Forest (RF) (Breiman, 2001) or Gradient Boosted Decision Trees (GBDT) (Friedman, 2001) are considered among the state-of-the-art models (Borisov et al., 2021). As a consequence, some recourse methods were developed to find recourses for tree ensembles (Tolomei et al., 2017; Lucic et al., 2022) where the non-differentiability prevents a direct application of the recourse objective in (1). To extend our method to tree-based classifiers, we also derive an IR expression for tree ensembles, and develop a method which computes low IR recourses for these models.



(a) Distilling a RF classifier (left) into a single tree (right). In the left panel, the RF classifier averages 30 decision trees, indicating that the final axis-aligned regions (not shown) are complicated functions of all 30 decision trees.

(b) Computing recourse for the RF model (right) based on the hypercubes (left). The circle has radius 2σ , i.e., it shows the region where 95% of recourse inaccuracies fall when $\sigma^2 = 0.025$. The input \mathbf{x} has IR ≈ 0.5 . The CE has IR ≈ 0.05 .

Figure 6: Computing certified recourses on the 2d Moon data set (Pedregosa et al., 2011) for a RF classifier. **Figure a):** Distilling a RF classifier (left panel) into a single decision tree (right panel) using knowledge distillation (Domingos, 1997). **Figure b):** Using the distilled tree, we form the hypercubes (left panel) required to compute IR according to Theorem 2. We then optimize (7) to find certified recourses for the RF model (right panel).

Tree Ensemble Classifiers An object of interest is the predicted output of a decision tree:

$$\mathcal{T}(\mathbf{x}) = \sum_{R \in \mathcal{R}_{\mathcal{T}}} c_{\mathcal{T}}(R) \cdot \mathbb{I}(\mathbf{x} \in R), \quad (8)$$

where $c_{\mathcal{T}}(R) \in \{0, 1\}$ is the constant prediction assigned in region $R \in \mathcal{R}_{\mathcal{T}}$ for tree \mathcal{T} . Moreover, a decision forest is formed by a set of M_T decision trees, and forms the probabilistic output:

$$f_{\text{Forest}}(\mathbf{x}) = \frac{1}{M_T} \sum_{m=1}^{M_T} \mathcal{T}_m(\mathbf{x}). \quad (9)$$

The predicted class of an input \mathbf{x} is formed via a vote by the trees where each tree assigns a probability estimate to the input. That is, the predicted class is the one with highest mean probability estimate across the trees. After the trees are combined, the multiple models form a single model again (Domingos, 1997). Thus, the corresponding predicted class of (9) is given by:

$$\mathcal{F}(\mathbf{x}) = \sum_{R \in \mathcal{R}_{\mathcal{F}}} c_{\mathcal{F}}(R) \cdot \mathbb{I}(\mathbf{x} \in R), \quad (10)$$

where $c_{\mathcal{F}}(R) \in \{0, 1\}$ is the constant prediction assigned in region $R \in \mathcal{R}_{\mathcal{F}}$ for the ensemble of trees \mathcal{F} . Furthermore, note that for each ensemble, there is an active subset of ensemble-specific features $\mathcal{S}_{\mathcal{F}} \subseteq \{1, \dots, d\}$ on which axis-aligned splits took place. Finally, we note that this formulation is quite general as it subsumes a large class of popular tree-based models such as Random Forests (RF) and Gradient Boosted Decision Trees (GBDT).

A.1 The Recourse IR for Tree Ensemble Classifiers

Theorem 2 (IR for Tree-Ensemble Classifiers). *Consider the decision forest classifier in (10). The recourse invalidation rate under Gaussian distributed response inconsistencies $\varepsilon \sim \mathcal{N}(\mathbf{0}, \sigma^2 \mathbf{I})$ is given by:*

$$\Delta(\tilde{\mathbf{x}}_E; \Sigma) = 1 - \sum_{R \in \mathcal{R}_{\mathcal{F}}} c_{\mathcal{F}}(R) \prod_{j \in \mathcal{S}_{\mathcal{F}}} d_{j,R}(\tilde{x}_{E,j}), \quad (11)$$

where

$$d_{j,R}(\tilde{x}_{E,j}) = \left[\Phi\left(\frac{\bar{t}_{j,R} - \tilde{x}_{E,j}}{\sigma_j}\right) - \Phi\left(\frac{\underline{t}_{j,R} - \tilde{x}_{E,j}}{\sigma_j}\right) \right], \quad (12)$$

and where Φ is the Gaussian CDF, $\bar{t}_{j,R}$ and $\underline{t}_{j,R}$ are the upper and lower points corresponding to feature $j \in \mathcal{S}_{\mathcal{F}}$ that define the hypercube formed by region R .

Proof Sketch. The proof uses the insight that a decision forest based on trees with axis-aligned splits partitions the input space into hypercubes where the prediction is either 0 or 1. It then remains to evaluate Gaussian integrals subject to the constrains set by the hypercubes. The full proof is given in Appendix D.2. \square

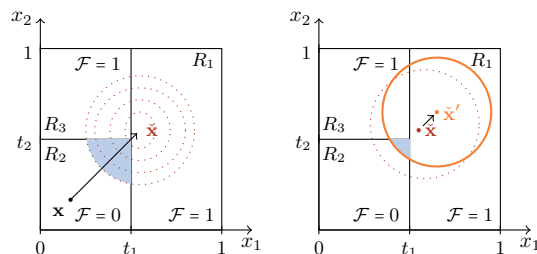
Below we provide a simple illustrative example of the result. Our proof of Theorem 2 assumed that the split points $\bar{t}_{j,R}$ and $\underline{t}_{j,R}$, corresponding to the tree-ensemble, are readily available. However, the hypercubes formed by the tree-ensemble, for which the prediction is constant, is a function of all individual trees, and of how they are combined. Thus, the clear-cut division into hypercubes present in each of the trees got lost in the process of model averaging.

Model Distillation to Evaluate IR We suggest a solution to this problem by using a technique called *model distillation* (Domingos, 1997; Bucilua et al., 2006; Hinton et al., 2015; Phuong & Lampert, 2019). In a nutshell: We wish to change the form of the model (to a simpler decision tree) while keeping the same knowledge (from our tree ensemble) (Hinton et al., 2015). Thus, the goal of this technique is to distil the knowledge of a larger model (possibly an ensemble) into a single, small (and interpretable) model. In our case, the ensemble is formed by decision trees, and the target model is a decision tree as well. Second, the method is simple to operationalize: let h be your complex model, and g denotes the simple model. Then we use our data $\{\mathbf{x}_i, y_i\}_{i=1}^n$ to train and validate the model h . The target model, however, is trained on samples from $\{\mathbf{x}_i, h(\mathbf{x}_i)\}_{i=1}^n$ to mimic the behaviour of the complex model. We refer to panels 1 to 3 in Figure 7 to gain some intuition on how this technique works on a non-linear 2-dimensional data set.

Next, we provide an illustrative example of the result in Theorem 2.

Example 1. Consider the example in Figure 7a. Then the invalidation rate can be expressed by: $\Delta_{\text{Forest}} =$

$$1 - \underbrace{\left[\Phi\left(\frac{1-\tilde{x}_1}{\sigma}\right) - \Phi\left(\frac{t_1-\tilde{x}_1}{\sigma}\right) \right] \cdot \left[\Phi\left(\frac{1-\tilde{x}_2}{\sigma}\right) - \Phi\left(\frac{0-\tilde{x}_2}{\sigma}\right) \right]}_{\text{Probability to land in Region } R_1} - \underbrace{\left[\Phi\left(\frac{t_1-\tilde{x}_1}{\sigma}\right) - \Phi\left(\frac{0-\tilde{x}_1}{\sigma}\right) \right] \cdot \left[\Phi\left(\frac{1-\tilde{x}_2}{\sigma}\right) - \Phi\left(\frac{t_2-\tilde{x}_2}{\sigma}\right) \right]}_{\text{Probability to land in Region } R_3}.$$



(a) IR is colored in blue (b) More reliable recourse

Figure 7: (a) Developing an intuition for IR on tree ensemble classifiers. A tree ensemble classifier splits the input space $[0, 1]^2$ into three regions R_1 , R_2 and R_3 , using split points t_1 and t_2 . The probability of invalidation is marked in blue and called $\Delta_{\text{Forest}}(\tilde{\mathbf{x}})$. (b) Using EXPECT, we can increase recourse robustness. We find a recourse $\tilde{\mathbf{x}}'$ by decreasing the invalidation region, i.e., $\Delta_{\text{Forest}}(\tilde{\mathbf{x}}) > \Delta_{\text{Forest}}(\tilde{\mathbf{x}}')$.

B Classification Models

In this section, we describe how the classification models were fitted. We have used CARLA’s built-in functionality to fit classifiers using PyTorch (Paszke et al., 2019). All models use a 80 – 20 train-test split for model training and evaluation. We evaluate model quality based on the model accuracy. All models are trained with the same architectures across the data sets:

	Neural Network	Logistic Regression
Units	[Input dim., 50, 2]	[Input dim., 2]
Type	Fully connected	Fully connected
Intermediate activations	ReLU	N/A
Last layer activations	Softmax	Softmax

Table 2: Classification model details

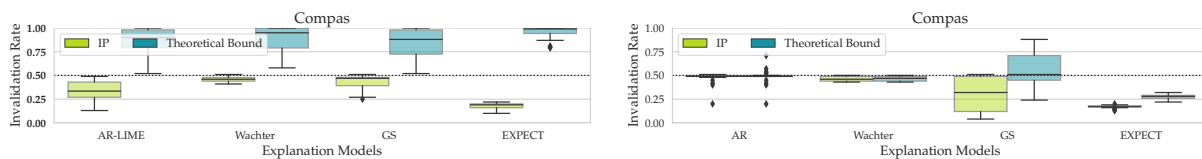
		Adult	COMPAS	Give Me Credit
Batch-size	NN	512	32	64
	Logistic Regression	512	32	64
Epochs	NN	50	40	30
	Logistic Regression	50	40	30
Learning rate	NN	0.002	0.002	0.001
	Logistic Regression	0.002	0.002	0.001

Table 3: Training details

	Adult	COMPAS	Give Me Credit
Logistic Regression	0.83	0.84	0.92
Neural Network	0.85	0.85	0.93

Table 4: Performance of models used for generating recourses

C Additional Experiments



(a) Logistic Regression (Left), NN (Right), $\sigma^2 = 0.01$

Figure 8: Missing figures from the main text.

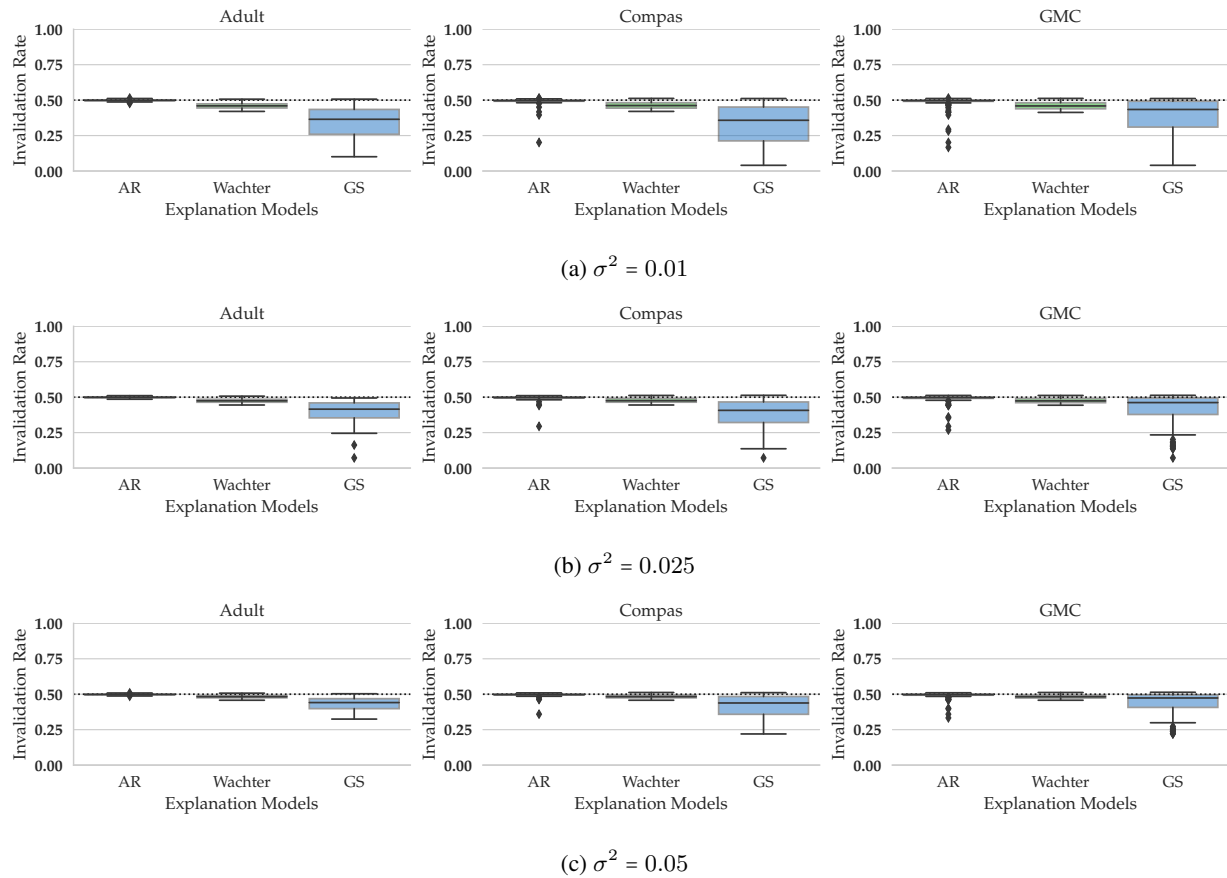


Figure 9: Boxplots of recourse invalidation probabilities across successfully generated recourses \check{x} for logistic regression classifiers on three data sets. The recourses were generated by three different explanation models (i.e., AR, Wachter, and GS), which use different techniques (i.e., integer programming, gradient search, and random search) to find minimum cost recourses. We perturbed the recourses by adding small normally distributed response inaccuracies $\varepsilon \sim \mathcal{N}(\mathbf{0}, \sigma^2 \cdot \mathbf{I})$ to \check{x} .

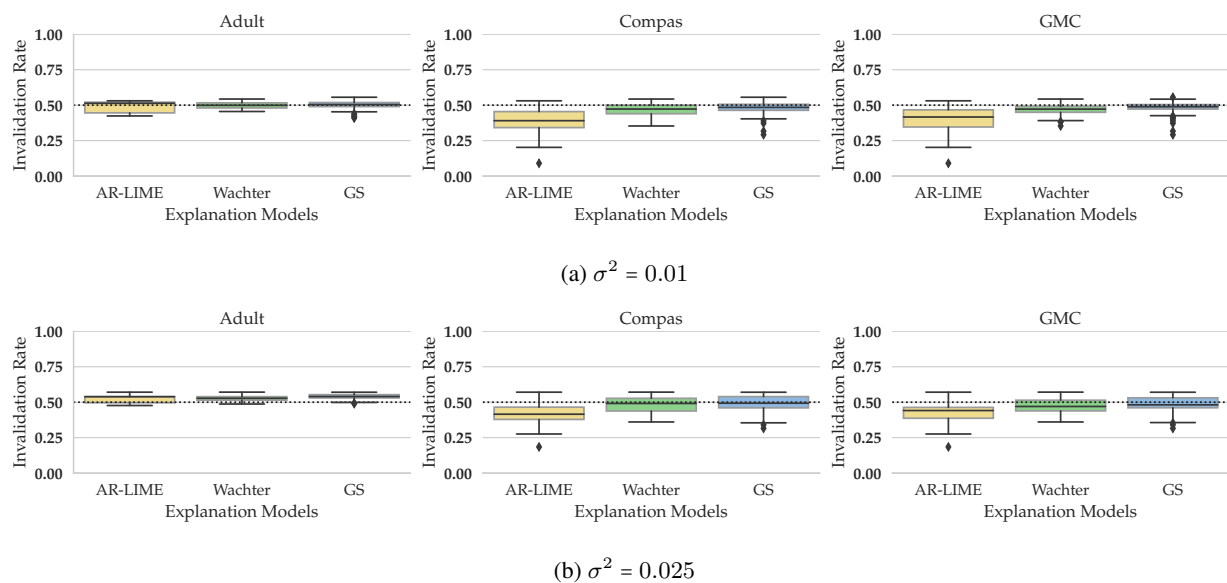


Figure 10: Boxplots of recourse invalidation probabilities across successfully generated recourses \check{x} for NN classifiers on three data sets. The recourses were generated by three different explanation models (i.e., AR-LIME, Wachter, and GS), which use different techniques (i.e., integer programming, gradient search, and random search) to find minimum cost recourses. We perturbed the recourses by adding small normally distributed response inaccuracies $\varepsilon \sim \mathcal{N}(\mathbf{0}, \sigma^2 \cdot \mathbf{I})$ to \check{x} .

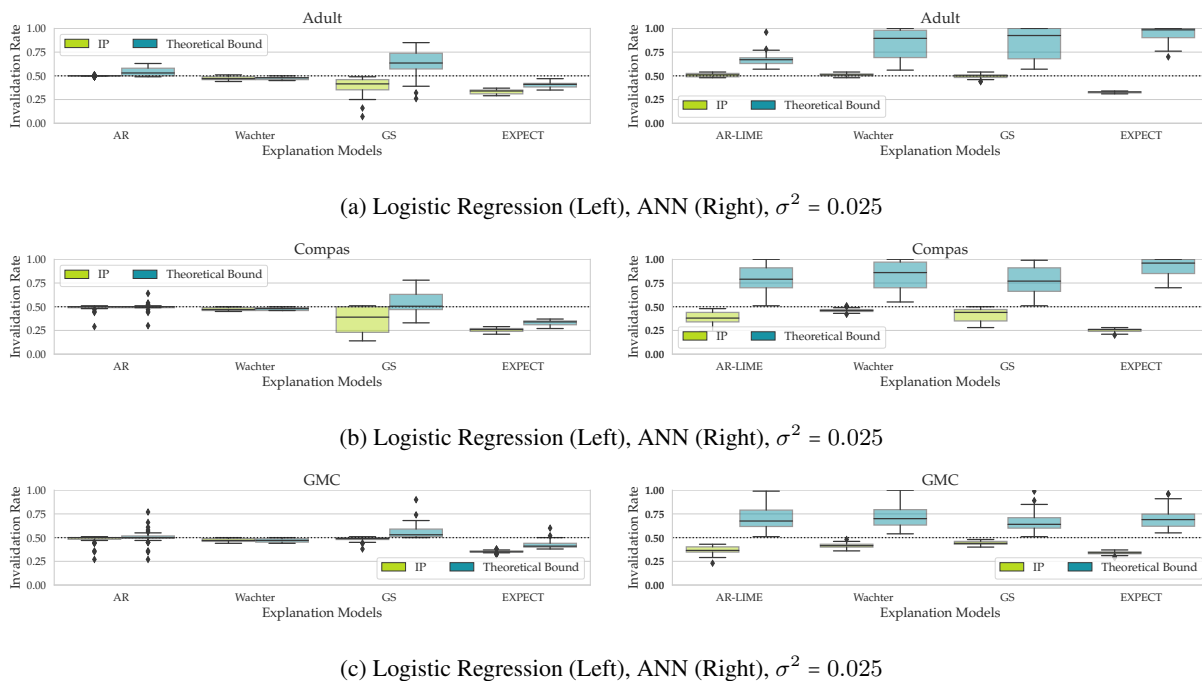


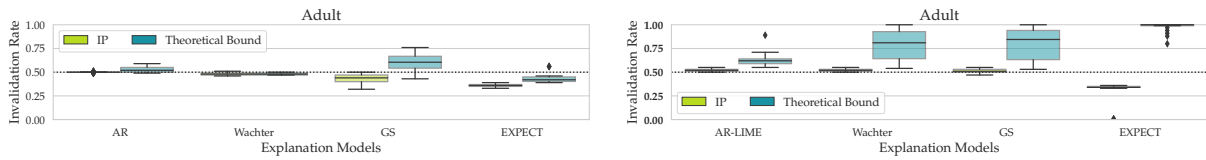
Figure 11: Verifying the theoretical upper bound from Lemma 2 for the logistic regression and artificial neural network classifiers on all data sets when $\sigma^2 = 0.025$. The green boxplots show the empirical recourse IRs for AR(-LIME), Wachter, GS, and EXPECT. The blue boxplots show the distribution of upper bounds, which we evaluated by plugging in the corresponding quantities (i.e., σ^2 , ω , etc.) into the upper bound from Lemma 2. The results show no violations of our theoretical bounds.

	Adult				Compas				GMC			
	AR	Wachter	GS	EXPECT	AR	Wachter	GS	EXPECT	AR	Wachter	GS	EXPECT
LR	0.98	1.0	1.0	1.0	1.0	1.0	1.0	1.0	1.0	1.0	1.0	1.0
AIR (\downarrow)	0.5 ± 0.01	0.48 ± 0.01	0.4 ± 0.08	0.28 ± 0.02	0.49 ± 0.03	0.48 ± 0.02	0.36 ± 0.14	0.17 ± 0.01	0.48 ± 0.04	0.47 ± 0.02	0.49 ± 0.02	0.3 ± 0.01
AC (\downarrow)	0.55 ± 0.4	0.62 ± 0.43	2.06 ± 1.03	2.21 ± 3.17	0.16 ± 0.17	0.22 ± 0.17	0.73 ± 0.45	0.68 ± 0.28	0.29 ± 0.27	0.49 ± 0.51	0.28 ± 0.32	1.22 ± 2.29
NN	0.38	1.0	1.0	1.0	0.84	1.0	1.0	1.0	0.4	1.0	1.0	1.0
AIR (\downarrow)	0.51 ± 0.02	0.51 ± 0.01	0.5 ± 0.02	0.33 ± 0.01	0.39 ± 0.06	0.46 ± 0.02	0.41 ± 0.07	0.25 ± 0.02	0.37 ± 0.05	0.42 ± 0.03	0.44 ± 0.02	0.34 ± 0.02
AC (\downarrow)	1.05 ± 0.22	0.3 ± 0.19	3.11 ± 1.62	1.98 ± 2.35	1.15 ± 0.52	0.2 ± 0.16	1.0 ± 0.17	0.84 ± 0.34	0.2 ± 0.16	0.26 ± 0.18	0.11 ± 0.09	0.41 ± 0.23

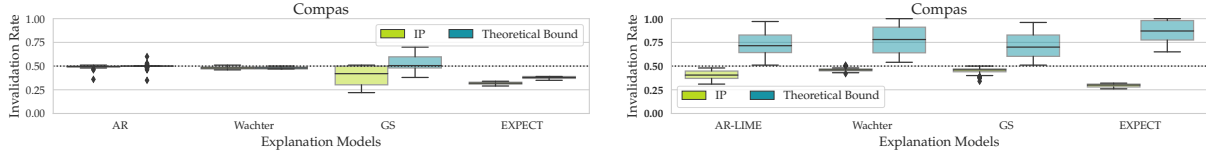
Table 5: Recourse accuracy (RA), average recourse invalidation rate (AIR) for $\sigma^2 = 0.025$ and average cost (AC) across different recourse methods. Recourses that use our framework EXPECT are more robust compared to those produced by existing baselines. For EXPECT, we generated recourses by setting $r = 0.35$ and $\sigma^2 = 0.01$. As a consequence, the AIR should be at most 0.35, which is in line with our results.

	Adult				Compas				GMC			
	AR	Wachter	GS	EXPECT	AR	Wachter	GS	EXPECT	AR	Wachter	GS	EXPECT
LR	0.98	1.0	1.0	1.0	1.0	1.0	1.0	1.0	1.0	1.0	1.0	1.0
AIR (\downarrow)	0.5 ± 0.01	0.48 ± 0.01	0.43 ± 0.05	0.31 ± 0.01	0.49 ± 0.01	0.49 ± 0.01	0.39 ± 0.1	0.23 ± 0.01	0.49 ± 0.03	0.48 ± 0.01	0.49 ± 0.02	0.32 ± 0.01
AC (\downarrow)	0.55 ± 0.4	0.62 ± 0.43	2.08 ± 1.0	3.15 ± 4.71	0.16 ± 0.17	0.22 ± 0.17	0.73 ± 0.45	0.72 ± 0.25	0.29 ± 0.27	0.49 ± 0.51	0.28 ± 0.31	6.96 ± 4.08
NN	0.38	1.0	1.0	0.66	0.84	1.0	1.0	1.0	0.38	1.0	1.0	1.0
AIR (\downarrow)	0.52 ± 0.01	0.52 ± 0.01	0.52 ± 0.02	0.3 ± 0.12	0.4 ± 0.04	0.46 ± 0.02	0.45 ± 0.04	0.29 ± 0.02	0.32 ± 0.04	0.39 ± 0.03	0.41 ± 0.02	0.35 ± 0.01
AC (\downarrow)	1.05 ± 0.22	0.3 ± 0.19	2.86 ± 1.6	32.1 ± 32.98	1.15 ± 0.52	0.2 ± 0.16	0.82 ± 0.45	0.88 ± 0.35	0.2 ± 0.19	0.26 ± 0.18	0.12 ± 0.1	0.35 ± 0.24

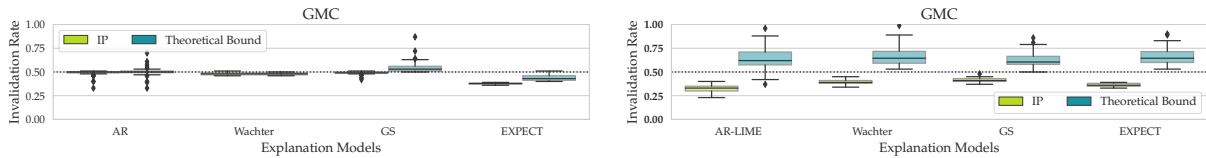
Table 6: Recourse accuracy (RA), average recourse invalidation rate (AIR) for $\sigma^2 = 0.05$ and average cost (AC) across different recourse methods. Recourses that use our framework EXPECT are more robust compared to those produced by existing baselines. For EXPECT, we generated recourses by setting $r = 0.35$ and $\sigma^2 = 0.01$. As a consequence, the AIR should be at most 0.35, which is in line with our results.



(a) Logistic Regression (Left), NN (Right), $\sigma^2 = 0.05$

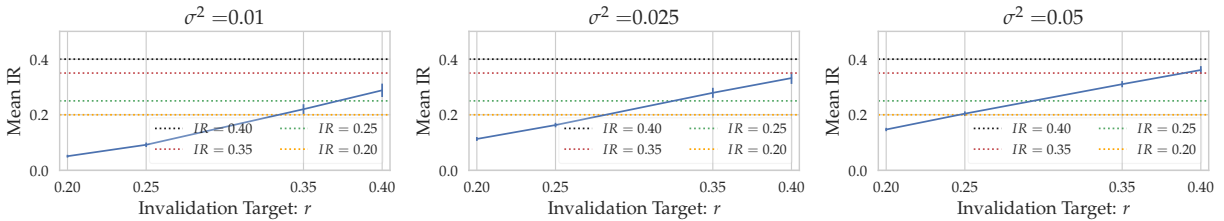


(b) Logistic Regression (Left), NN (Right), $\sigma^2 = 0.05$

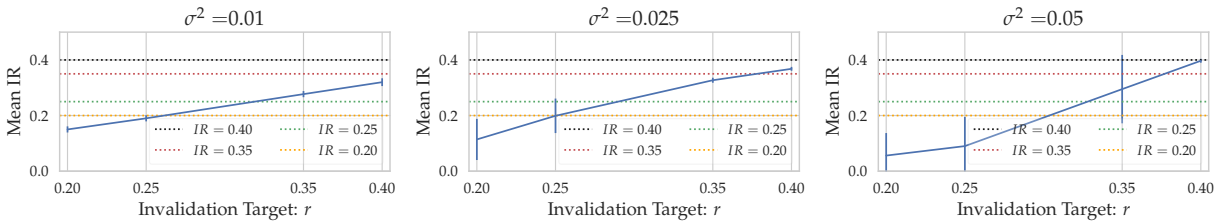


(c) Logistic Regression (Left), NN (Right), $\sigma^2 = 0.05$

Figure 12: Verifying the theoretical upper bound from Lemma 2 for the logistic regression and artificial neural network classifiers on all data set for $\sigma^2 = 0.05$. The green boxplots show the empirical recourse IRs for AR(-LIME), Wachter, GS, and EXPECT. The blue boxplots show the distribution of upper bounds, which we evaluated by plugging in the corresponding quantities (i.e., σ^2 , ω , etc.) into the upper bound from Lemma 2. The results show no violations of our theoretical bounds.



(a) LR



(b) NN

Figure 13: Verifying that the invalidation rate for our framework EXPECT (blue line) is at most equal to the invalidation target r on the Adult data set for different $\sigma^2 \in \{0.01, 0.025, 0.05\}$ across both classifiers. We compute the *mean IR* across every instance in the test set. To do that, we sample 10,000 points from $\epsilon \sim \mathcal{N}(\mathbf{0}, \sigma^2 \mathbf{I})$ for every instance and compute IR in (2). Then the *mean IR* quantifies recourse robustness where the individual IRs are averaged over all instances from the test set. The vertical bars indicate the corresponding standard deviations.

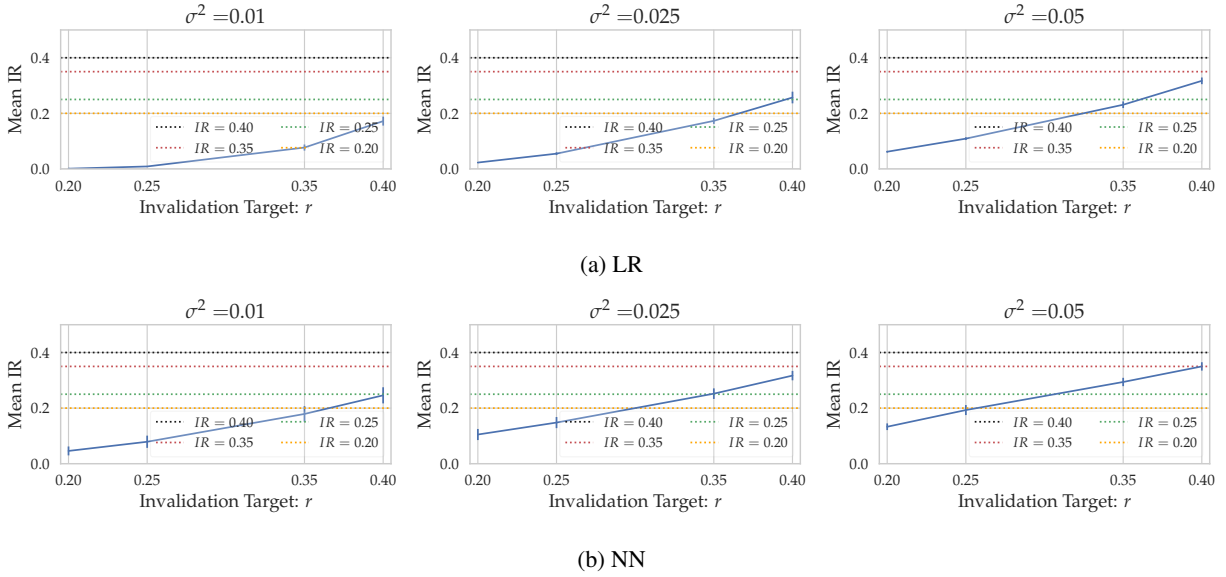


Figure 14: Verifying that the invalidation rate for our framework EXPECT (blue line) is at most equal to the invalidation target r on the Compas data set for different $\sigma^2 \in \{0.01, 0.025, 0.05\}$ across both classifiers. We compute the *mean IR* across every instance in the test set. To do that, we sample 10,000 points from $\varepsilon \sim \mathcal{N}(\mathbf{0}, \sigma^2 \mathbf{I})$ for every instance and compute IR in (2). Then the *mean IR* quantifies recourse robustness where the individual IRs are averaged over all instances from the test set. The vertical bars indicate the corresponding standard deviations.

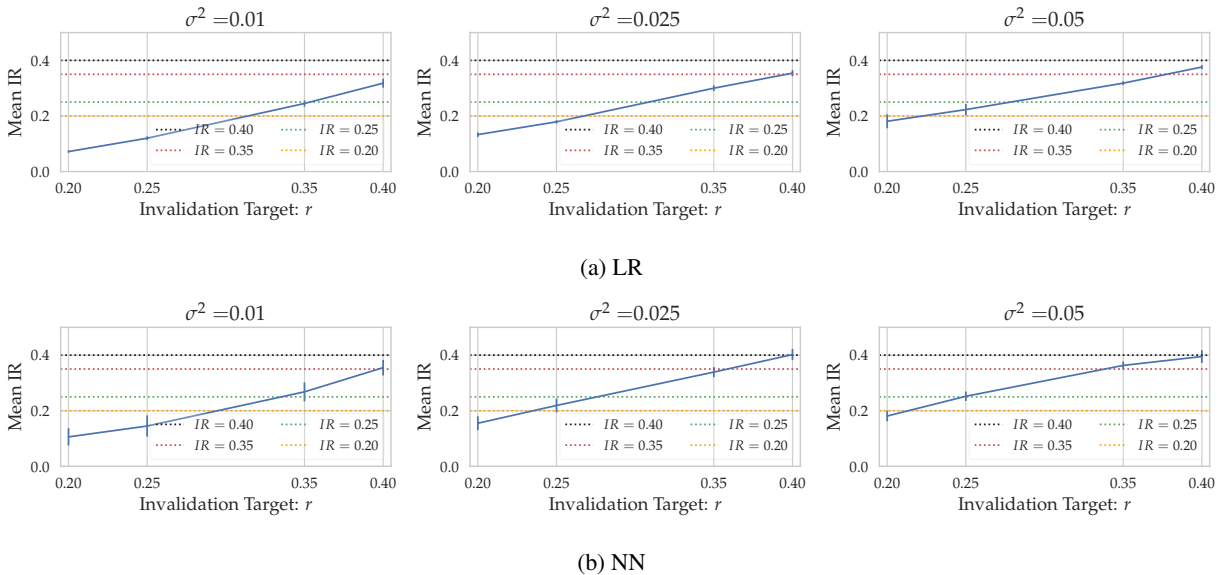


Figure 15: Verifying that the invalidation rate for our framework EXPECT (blue line) is at most equal to the invalidation target r on the GMC data set for different $\sigma^2 \in \{0.01, 0.025, 0.05\}$ across both classifiers. We compute the *mean IR* across every instance in the test set. To do that, we sample 10,000 points from $\varepsilon \sim \mathcal{N}(\mathbf{0}, \sigma^2 \mathbf{I})$ for every instance and compute IR in (2). Then the *mean IR* quantifies recourse robustness where the individual IRs are averaged over all instances from the test set. The vertical bars indicate the corresponding standard deviations.

D Proofs

D.1 Proof of Theorem 1

Theorem 1. A first-order approximation $\tilde{\Delta}$ to the recourse invalidation rate Δ in (2) under a Gaussian distribution $\varepsilon \sim \mathcal{N}(\mathbf{0}, \Sigma)$ capturing the noise in human responses is given by:

$$\tilde{\Delta}(\check{\mathbf{x}}_E; \Sigma) = 1 - \Phi\left(\frac{f(\check{\mathbf{x}}_E)}{\sqrt{\nabla f(\check{\mathbf{x}}_E) \Sigma \nabla f(\check{\mathbf{x}}_E)^T}}\right), \quad (13)$$

where Φ is the CDF of the univariate standard normal distribution $\mathcal{N}(0, 1)$, $f(\check{\mathbf{x}}_E)$ denotes the logit score at $\check{\mathbf{x}}_E$ which is the recourse output by a recourse method E , and $h(\check{\mathbf{x}}_E) \in \{0, 1\}$.

Proof. Let the random variable ε follow a multivariate normal distribution, i.e., $\varepsilon \sim \mathcal{N}(\boldsymbol{\mu}, \Sigma)$. The following result is a well-known fact: $\mathbf{v}^T \varepsilon \sim \mathcal{N}(\mathbf{v}^T \boldsymbol{\mu}, \mathbf{v} \Sigma \mathbf{v}^T)$ where $\mathbf{v} \in \mathbb{R}^d$. Let \mathbf{x} denote the input sample for which we wish to find a counterfactual $\check{\mathbf{x}}_E = \mathbf{x} + \boldsymbol{\delta}_E$. Recall from Definition 1 that we have to evaluate:

$$\begin{aligned} \Delta &= \mathbb{E}_\varepsilon \left[\underbrace{h(\check{\mathbf{x}}_E)}_{\text{CE class}} - \underbrace{h(\check{\mathbf{x}}_E + \varepsilon)}_{\text{class after response}} \right] \\ &= 1 - \mathbb{E}_\varepsilon [h(\check{\mathbf{x}}_E + \varepsilon)], \end{aligned} \quad (14)$$

where we have used that the first term is a constant and evaluates to 1 by the definition of a counterfactual explanation. It remains to evaluate the expectation: $\mathbb{E}_\varepsilon [h(\check{\mathbf{x}}_E + \varepsilon)]$. Next, we note that (14) can equivalently be expressed in terms of the logit outcomes:

$$\Delta = \mathbb{E}_\varepsilon \left[\underbrace{\mathbb{I}[f(\check{\mathbf{x}}_E) > 0]}_{\text{CE class}} - \underbrace{\mathbb{I}[f(\check{\mathbf{x}}_E + \varepsilon) > 0]}_{\text{class after perturbation}} \right] = \left(1 - \mathbb{E}_\varepsilon [\mathbb{I}[f(\check{\mathbf{x}}_E + \varepsilon) > 0]] \right). \quad (15)$$

Again, we are interested in the second term, which evaluates to:

$$\mathbb{E}_\varepsilon [\mathbb{I}[f(\check{\mathbf{x}}_E + \varepsilon) > 0]] = 0 \cdot \mathbb{P}\left(f(\check{\mathbf{x}}_E + \varepsilon) < 0\right) + 1 \cdot \mathbb{P}\left(f(\check{\mathbf{x}}_E + \varepsilon) > 0\right). \quad (16)$$

Next, consider the first-order Taylor approximation: $f(\check{\mathbf{x}}_E + \varepsilon) \approx f(\check{\mathbf{x}}_E) + \nabla f(\check{\mathbf{x}}_E)^T \varepsilon$. Hence, we know $\nabla f(\check{\mathbf{x}}_E)^T \varepsilon$ approximately follows $\mathcal{N}(\mathbf{0}, \nabla f(\check{\mathbf{x}}_E) \Sigma \nabla f(\check{\mathbf{x}}_E)^T)$. Now, the second term can be computed as follows:

$$\begin{aligned} \mathbb{P}\left(f(\check{\mathbf{x}}_E + \varepsilon) > 0\right) &\approx \mathbb{P}\left(f(\check{\mathbf{x}}_E) + \nabla f(\check{\mathbf{x}}_E)^T \varepsilon > 0\right) = \mathbb{P}\left(-f(\check{\mathbf{x}}_E) < \nabla f(\check{\mathbf{x}}_E)^T \varepsilon\right) \\ &= 1 - \mathbb{P}\left(-f(\check{\mathbf{x}}_E) > \nabla f(\check{\mathbf{x}}_E)^T \varepsilon\right) = 1 - \mathbb{P}\left(\underbrace{\frac{\nabla f(\check{\mathbf{x}}_E)^T \varepsilon}{\sqrt{\nabla f(\check{\mathbf{x}}_E) \Sigma \nabla f(\check{\mathbf{x}}_E)^T}}}_{\text{Mean 0 Gaussian RV}} < \underbrace{-\frac{f(\check{\mathbf{x}}_E)}{\sqrt{\nabla f(\check{\mathbf{x}}_E) \Sigma \nabla f(\check{\mathbf{x}}_E)^T}}}_{\text{Constant}}\right) \\ &= 1 - \Phi\left(-\frac{f(\check{\mathbf{x}}_E)}{\sqrt{\nabla f(\check{\mathbf{x}}_E) \Sigma \nabla f(\check{\mathbf{x}}_E)^T}}\right) \\ &= \Phi\left(\frac{f(\check{\mathbf{x}}_E)}{\sqrt{\nabla f(\check{\mathbf{x}}_E) \Sigma \nabla f(\check{\mathbf{x}}_E)^T}}\right), \end{aligned} \quad (17)$$

where the last line follows due to symmetry of the standard normal distribution (i.e., $\Phi(-u) = 1 - \Phi(u)$). Putting the pieces together, we have:

$$\mathbb{E}_\varepsilon [\mathbb{I}[f(\check{\mathbf{x}}_E + \varepsilon) > 0]] = 0 \cdot \mathbb{P}\left(f(\check{\mathbf{x}}_E + \varepsilon) < 0\right) + 1 \cdot \mathbb{P}\left(f(\check{\mathbf{x}}_E + \varepsilon) \geq 0\right) \quad (19)$$

$$= \Phi\left(\frac{f(\check{\mathbf{x}}_E)}{\sqrt{\nabla f(\check{\mathbf{x}}_E) \Sigma \nabla f(\check{\mathbf{x}}_E)^T}}\right). \quad (20)$$

Thus, we have:

$$\Delta \approx \tilde{\Delta} = 1 - \Phi\left(\frac{f(\tilde{\mathbf{x}}_E)}{\sqrt{\nabla f(\tilde{\mathbf{x}}_E)\Sigma\nabla f(\tilde{\mathbf{x}}_E)^T}}\right), \quad (21)$$

which completes our proof. Note that this is equivalent to $\mathbb{P}\left(f(\tilde{\mathbf{x}}_E + \varepsilon) < 0\right)$, and thus we are ‘‘counting’’ how often perturbations to $\tilde{\mathbf{x}}_E$ sampled from $\varepsilon \sim \mathcal{N}(\mathbf{0}, \Sigma)$ result in flips back to the undesired class. \square

Lemma 2. *Let $\tilde{\mathbf{x}}_E$ be the output produced by some recourse method E such that $h(\tilde{\mathbf{x}}_E) = 1$. Then, an upper bound on $\tilde{\Delta}$ from (3) is given by:*

$$\tilde{\Delta}(\tilde{\mathbf{x}}_E; \sigma^2\mathbf{I}) \leq 1 - \Phi\left(c + \frac{\omega}{\sigma} \frac{\|\nabla f(\mathbf{x})\|_2}{\|\nabla f(\tilde{\mathbf{x}}_E)\|_2} \frac{\|\delta_E\|_1}{\sqrt{\|\delta_E\|_0}}\right), \quad (22)$$

where $c = \frac{f(\mathbf{x})}{\sigma\|\nabla f(\mathbf{x})\|_2}$ is a constant, $\delta_E = \tilde{\mathbf{x}}_E - \mathbf{x}$, and $\omega > 0$ is the cosine of the angle between the vectors $\nabla f(\mathbf{x})$ and δ_E .

Proof. We start by noting the following basic inequality:

$$\|\mathbf{z}\|_1 \leq \sqrt{\|\mathbf{z}\|_0} \cdot \|\mathbf{z}\|_2.$$

Going forward, we will refer to these inequalities as basic inequalities. Moreover, note that Φ is a monotonic function. Thus, we have $\Phi(a) \leq \Phi(a')$ for $a \leq a'$. Note that $f(\tilde{\mathbf{x}}_E) \approx f(\mathbf{x}) + \nabla f(\mathbf{x})^T \delta_E$. Thus we obtain the following approximation:

$$\tilde{\Delta} = 1 - \Phi\left(\frac{f(\mathbf{x}) + \nabla f(\mathbf{x})^T \delta_E}{\sqrt{\nabla f(\tilde{\mathbf{x}}_E)\Sigma\nabla f(\tilde{\mathbf{x}}_E)^T}}\right). \quad (23)$$

Next, we will find upper bounds for the term on the right: Before we will do that, we will express the above expression more conveniently to highlight the impact of the counterfactual action δ_E more explicitly. To do that, note that $\nabla f(\mathbf{x})^T \delta_E = \omega \cdot \|\nabla f(\mathbf{x})\|_2 \cdot \|\delta_E\|_2$ where ω is the cosine of the angle between the vectors $\nabla f(\mathbf{x})$ and δ_E . Using $\Sigma = \sigma^2\mathbf{I}$, we obtain:

$$\Phi\left(\frac{f(\mathbf{x}) + \nabla f(\mathbf{x})^T \delta_E}{\sigma\|\nabla f(\tilde{\mathbf{x}}_E)\|_2}\right) = \Phi\left(c + \frac{\|\nabla f(\mathbf{x})\|_2}{\|\nabla f(\tilde{\mathbf{x}}_E)\|_2} \cdot \frac{\omega}{\sigma} \cdot \|\delta_E\|_2\right), \quad (24)$$

where we defined a constant $c = \frac{f(\mathbf{x})}{\sigma\|\nabla f(\tilde{\mathbf{x}}_E)\|_2}$ using quantities that we will keep fixed in our analysis, namely \mathbf{x} , $\nabla f(\mathbf{x})$ and σ . Also note that \mathbf{x} is the factual input, and thus its logit score satisfies: $f(\mathbf{x}) < 0$. Since δ_E is a valid perturbation, we must have that $\omega > 0$ for the perturbation to change the class prediction.

Note that the following *lower bound* holds by the basic inequality stated above:

$$\Phi\left(c + \frac{\|\nabla f(\mathbf{x})\|_2}{\|\nabla f(\tilde{\mathbf{x}}_E)\|_2} \cdot \frac{\omega}{\sigma} \cdot \|\delta_E\|_2\right) \geq \Phi\left(c + \frac{\|\nabla f(\mathbf{x})\|_2}{\|\nabla f(\tilde{\mathbf{x}}_E)\|_2} \cdot \frac{\omega}{\sigma} \cdot \frac{\|\delta_E\|_1}{\sqrt{\|\delta_E\|_0}}\right). \quad (25)$$

As a consequence we obtain the following *upper bound on the IR*:

$$\tilde{\Delta} \leq 1 - \Phi\left(c + \frac{\|\nabla f(\mathbf{x})\|_2}{\|\nabla f(\tilde{\mathbf{x}}_E)\|_2} \cdot \frac{\omega}{\sigma} \cdot \frac{\|\delta_E\|_1}{\sqrt{\|\delta_E\|_0}}\right), \quad (26)$$

as claimed. \square

Lemma 1. *For the logistic regression classifier, consider the recourse output by Wachter et al. (2018): $\tilde{\mathbf{x}}_{\text{Wachter}}(s) = \mathbf{x} + \frac{s-f(\mathbf{x})}{\|\nabla f(\mathbf{x})\|_2} \nabla f(\mathbf{x})$. Then the recourse invalidation rate has the following closed-form:*

$$\Delta(\tilde{\mathbf{x}}_{\text{Wachter}}(s); \sigma^2\mathbf{I}) = 1 - \Phi\left(\frac{s}{\sigma\|\nabla f(\mathbf{x})\|_2}\right), \quad (27)$$

where s is the target logit score.

Proof. Since we are in the linear case, we have: $\nabla f(\check{\mathbf{x}}_E) = \nabla f(\mathbf{x})$. Also, note that $f(\check{\mathbf{x}}_E) = f(\mathbf{x}) + \nabla f(\mathbf{x})^T \boldsymbol{\delta}_E$. Using $\boldsymbol{\Sigma} = \sigma^2 \mathbf{I}$, we obtain the following exact expression:

$$\Delta = 1 - \Phi\left(\frac{f(\mathbf{x}) + \nabla f(\mathbf{x})^T \boldsymbol{\delta}_E}{\sigma \|\nabla f(\mathbf{x})\|_2}\right). \quad (28)$$

From Pawelczyk et al. (2022), we have:

$$\boldsymbol{\delta}_{\text{Wachter}} = \frac{s - f(\mathbf{x})}{\|\nabla f(\mathbf{x})\|_2^2} \nabla f(\mathbf{x}). \quad (29)$$

Plugging (29) into (28) we obtain:

$$\begin{aligned} \Delta &= 1 - \Phi\left(\frac{f(\mathbf{x})}{\sigma \|\nabla f(\mathbf{x})\|_2} + \frac{\nabla f(\mathbf{x})^T \boldsymbol{\delta}_E}{\sigma \|\nabla f(\mathbf{x})\|_2}\right) \\ &= 1 - \Phi\left(\frac{f(\mathbf{x})}{\sigma \|\nabla f(\mathbf{x})\|_2} + \frac{1}{\sigma \|\nabla f(\mathbf{x})\|_2} \cdot \nabla f(\mathbf{x})^T \nabla f(\mathbf{x}) \frac{s - f(\mathbf{x})}{\|\nabla f(\mathbf{x})\|_2^2}\right) \\ &= 1 - \Phi\left(\frac{f(\mathbf{x})}{\sigma \|\nabla f(\mathbf{x})\|_2} + \frac{s - f(\mathbf{x})}{\sigma \|\nabla f(\mathbf{x})\|_2}\right) \\ &= 1 - \Phi\left(\frac{s}{\sigma \|\nabla f(\mathbf{x})\|_2}\right), \end{aligned} \quad (30)$$

$$\quad (31)$$

which concludes the proof. \square

D.2 Proof of Theorem 2

Proof. From Definition 1 we know:

$$\Delta_{\text{Forest}} = \mathbb{E}_{\boldsymbol{\varepsilon}} \left[\underbrace{\mathcal{F}(\check{\mathbf{x}}_E)}_{\text{CE class}} - \underbrace{\mathcal{F}(\check{\mathbf{x}}_E + \boldsymbol{\varepsilon})}_{\text{class after response}} \right] \quad (32)$$

$$= 1 - \mathbb{E}_{\boldsymbol{\varepsilon}} [\mathcal{F}(\check{\mathbf{x}}_E + \boldsymbol{\varepsilon})]. \quad (33)$$

It remains to evaluate: $\mathbb{E}_{\boldsymbol{\varepsilon}} [\mathcal{F}(\check{\mathbf{x}}_E + \boldsymbol{\varepsilon})]$. Using (10), we have:

$$\begin{aligned} \mathbb{E}_{\boldsymbol{\varepsilon}} [\mathcal{F}(\check{\mathbf{x}}_E + \boldsymbol{\varepsilon})] &= \mathbb{E}_{\boldsymbol{\varepsilon}} \left[\sum_{R \in \mathcal{R}_{\mathcal{F}}} c_{\mathcal{F}}(R) \cdot \mathbb{I}(\check{\mathbf{x}}_E + \boldsymbol{\varepsilon} \in R) \right] \\ &= \sum_{R \in \mathcal{R}_{\mathcal{F}}} c_{\mathcal{F}}(R) \cdot \mathbb{E}_{\boldsymbol{\varepsilon}} [\mathbb{I}(\check{\mathbf{x}}_E + \boldsymbol{\varepsilon} \in R)] && \text{(Linearity of Expectation)} \\ &= \sum_{R \in \mathcal{R}_{\mathcal{F}}} c_{\mathcal{F}}(R) \cdot \int_{\mathcal{R}} p(\mathbf{y}) d\mathbf{y} && (p(\mathbf{y}) = \mathcal{N}(\check{\mathbf{x}}_E, \boldsymbol{\sigma}^2 \mathbf{I})) \\ &= \sum_{R \in \mathcal{R}_{\mathcal{F}}} c_{\mathcal{F}}(R) \cdot \prod_{j \in \mathcal{S}_{\mathcal{F}}} \int_{R_j} \frac{1}{\sqrt{2\pi\sigma_j^2}} \exp\left(-\frac{1}{2} \frac{(y_j - \check{x}_{E,j})^2}{\sigma_j^2}\right) dy_j \\ & && \text{(Since } \boldsymbol{\varepsilon} \text{ is an independent Gaussian)} \\ &= \sum_{R \in \mathcal{R}_{\mathcal{F}}} c_{\mathcal{F}}(R) \cdot \prod_{j \in \mathcal{S}_{\mathcal{F}}} \left[\Phi\left(\frac{\bar{t}_{j,R} - \check{x}_{E,j}}{\sigma_j}\right) - \Phi\left(\frac{\underline{t}_{j,R} - \check{x}_{E,j}}{\sigma_j}\right) \right]. && \text{(Since } \boldsymbol{\varepsilon} \text{ is Gaussian)} \end{aligned} \quad (34)$$

Using our Definition of robustness, we have

$$\Delta_{\text{Forest}} = 1 - \sum_{R \in \mathcal{R}_{\mathcal{F}}} c_{\mathcal{F}}(R) \prod_{j \in \mathcal{S}_{\mathcal{F}}} \left[\Phi\left(\frac{\bar{t}_{j,R} - \check{x}_{E,j}}{\sigma_j}\right) - \Phi\left(\frac{\underline{t}_{j,R} - \check{x}_{E,j}}{\sigma_j}\right) \right], \quad (35)$$

which completes the proof. \square